Field and Technical Report

THE FORMATION OF AN EARLY ACHEULEAN ARTEFACT-BEARING HORIZON ACROSS THE MAROPENG LANDSCAPE, CRADLE OF HUMANKIND, SOUTH AFRICA

PETER MORRISSEY[1*], ROSA M. MOLL[2] & DOMINIC J. STRATFORD[1,3]

[1]*School of Geography, Archaeology and Environmental Studies, University of the Witwatersrand, Private Bag 3, Wits 2050, South Africa*

Corresponding author. Email:* ***peter.morrissey@wits.ac.za*

[2]*Evolutionary Studies Institute, University of the Witwatersrand, Private Bag 3, Wits 2050, South Africa*

[3]*Department of Anthropology, Stony Brook University, Stony Brook, 11794-4364 NY, USA*

(Received September 2024. Revised February 2025)

ABSTRACT

Maropeng is the only published open-air Earlier Stone Age site within the Cradle of Humankind, an area renowned for its fossiliferous and artefact-bearing cave deposits. The excavation of Early Acheulean lithic assemblages from Maropeng offers an opportunity to study hominin behaviour in a context where evidence for landscape use may be preserved away from the better-known Cradle karstic environments. However, the assemblages are in secondary context and have been modified significantly by multiscale and long-term site formation processes, resulting in the formation of an artefact-bearing clast-supported buried pavement that extends over a significant area and varies considerably in thickness, clast size, and artefact abundance. Previous interpretations of its formation derive from the study of sedimentary profiles exposed in several small archaeological excavations in a limited area of the Maropeng landscape. Here, we apply a multiscale geoarchaeological approach within the geomorphological context of the landscape to clarify: a) the general formation of the artefact-bearing horizon at the landscape scale; b) variability in formation processes across this landscape; and c) the impact of site-scale depositional and post-depositional processes on the M2 assemblage, which has undergone detailed technological analysis. Results indicate that clasts were transported by slopewash along a saddle in the centre of the property from a quartzite ridge to the east, with some material subsequently moving downslope on either side of the saddle (north and south). Once deposited, these clast-rich deposits were winnowed to varying degrees, creating a deflated, clast-supported pavement that was subsequently buried. The horizon's extensive distribution and the heterogeneity of artefact abrasion states indicate that hominins discarded artefacts at various points on the landscape. The M2 excavation assemblage has been time-averaged and heavily modified by transport and winnowing but can still yield useful information on technological practices of Earlier Stone Age hominins at Maropeng.

Keywords: site formation, geoarchaeology, landscape archaeology, geomorphology, Early Acheulean, Cradle of Humankind

INTRODUCTION

Maropeng is located within the Cradle of Humankind (CoH) World Heritage Site, South Africa, less than 10 km north-west of the Sterkfontein Caves and Swartkrans (Fig. 1). It is the only published open-air Earlier Stone Age (ESA) site within the CoH (Pollarolo *et al.* 2010), and one of only two in the area (Caruana *et al.* 2019). ESA assemblages have been found at eight sites within the CoH and have been attributed to either the Oldowan or the Early Acheulean based on techno-typological analysis (Kuman 2003, 2007, 2016; Kuman & Field 2009; Lotter & Kuman 2018). Seven of the eight sites represent secondary-context accumulations of lithic artefacts in deposits within karstic cave networks (Lotter & Kuman 2018). To date, the only CoH ESA assemblages that have been extensively studied and published are those from Sterkfontein and Swartkrans (Kuman 2003, 2007; Kuman & Field 2009; Caruana 2017; Kuman *et al.* 2018). These lithic assemblages have been modified by a combination of processes including exposure on the surface (with the resulting potential for removal and/or dispersal of material), transport of artefacts by slopewash into the caves, and the post-depositional geogenic movement of material within the caves themselves (e.g. Brain 1993; Kuman 1994; Sutton *et al.* 2009; Stratford *et al.* 2012; Stratford *et al.* 2014; Stratford 2017).

Landscape-scale archaeology is an important tool in the study of the cognitive and social evolution of hominins during the ESA (Schick 1987; Blumenschine & Masao 1991; Plummer 2004). How hominins utilised space in relation to landscape features and associated resources is believed to be directly related to their cognitive abilities, especially their capacity for planning and organisation (Schick 1987; Potts 1991; Braun *et al.* 2008). For example, the relationship between distances to raw material sources and lithic reduction intensities has been investigated to identify the presence or absence of behavioural adaptations aimed at conserving energy and/or raw material (e.g. Blumenschine *et al.* 2008; Braun *et al.* 2008). Unfortunately, the deposition of lithic assemblages into the keyhole sites in the CoH prevents any meaningful understanding of spatial patterns in the use of the landscape around the cave entrances.

The CoH cave sites are sometimes compared unfavourably to open-air ESA sites and site complexes preserved in the East African Rift Valley (e.g. Kuman 1994, 2007) because the latter sites can be correlated stratigraphically or chronostratigraphically across palaeolandscapes utilising chronologically well-constrained volcanic tuff marker beds. The relatively high-resolution chronological control of East African assemblages, and the ability to contextualise the sites within broader environments based on geological evidence, has allowed the proposal of nuanced interpretations of ESA hominin behaviour in relation to the distribution of resources like water and lithic raw materials (e.g. Potts 1991; Plummer 2004; Blumenschine *et al.* 2008; Braun *et al.* 2008; Maurin *et al.* 2017). Unlike with processes relating to the caves, the accumulation, preservation, and integrity of the Rift assemblages are largely controlled by landscape geomorphological evolution.

The archaeological significance of Maropeng was first recognised in 2005 when lithic artefacts were noticed by Kathleen Kuman and Ronald Clarke in construction cuttings (Pollarolo *et al.* 2010). Several small excavations were conducted around the marketplace (Fig. 2) to collect a contextualised sample of artefacts, while a larger number of lithics were obtained from construction dump piles (Pollarolo *et al.* 2010). Analysis of both assemblages

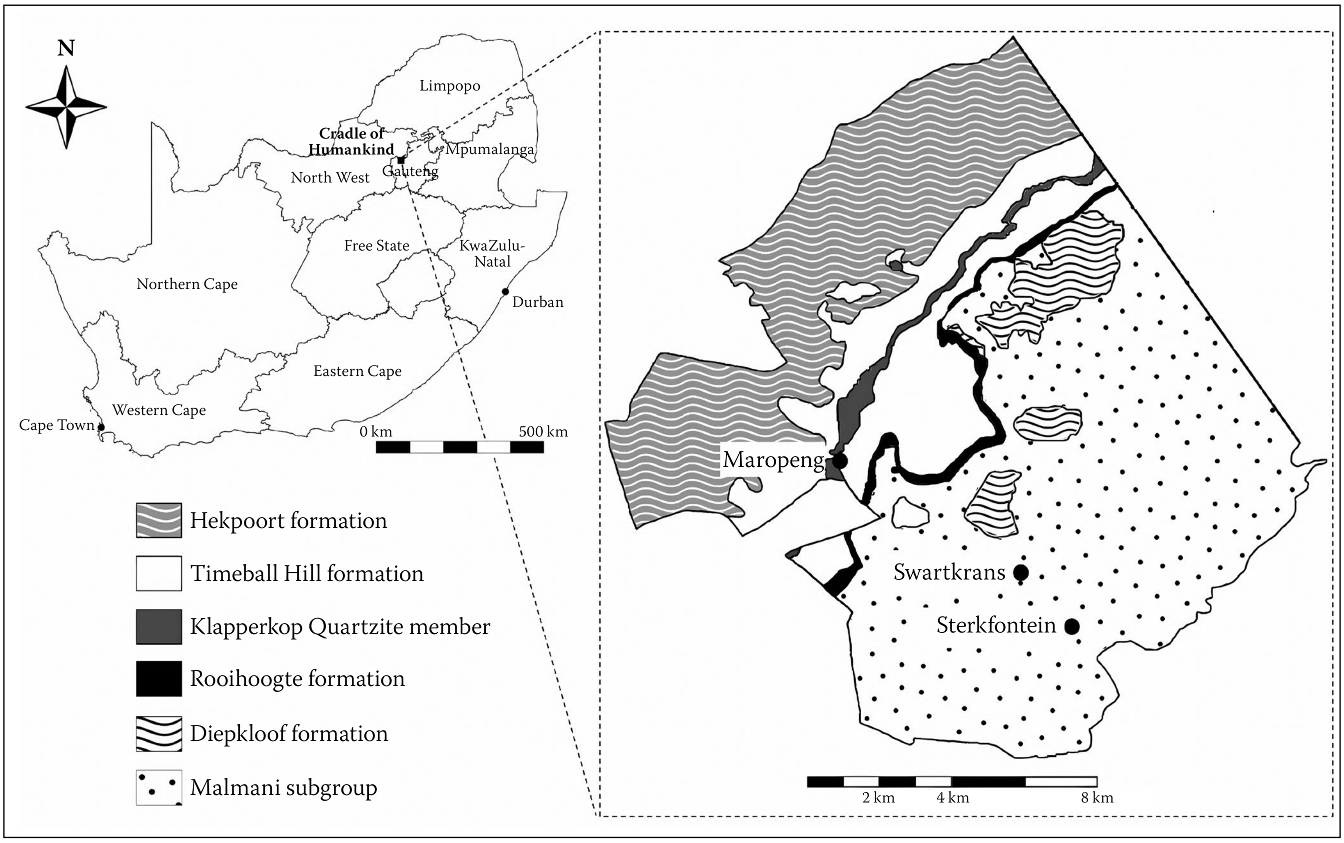

FIG. 1. *Left: Map of the Republic of South Africa, with the Cradle of Humankind indicated. Right: Geological map of the area around Maropeng, Swartkrans and Sterkfontein (modified from Leyland 2008).*

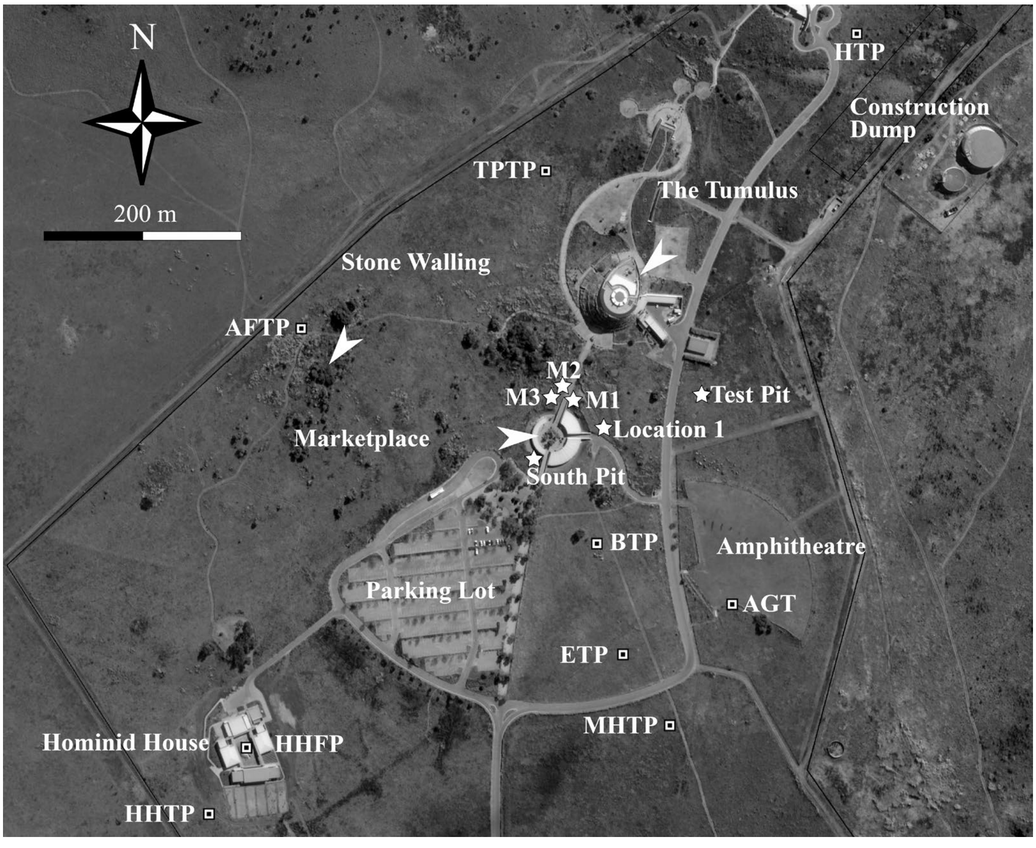

FIG. 2. *Map of the study area (Imagery: Google Earth 2016). Buildings and other features constructed during recent development are indicated. Note the Iron Age stone walling to the west. Excavations conducted by Pollarolo* **et al.** *(2010) and those led by Stratford are marked with white stars. The locations of the test pits (HHTP, HHFP, MHTP, ETP, BTP, AFTP, TPTP, HTP) and geotrench (AGT) excavated for this study are marked with white squares. Data from the M2 excavation site were also utilised in the study. Note that Pollarolo* **et al.***'s (2010) Location 2 and western test pit are shown as M1 and M3, respectively, their new designations following their expansion during Stratford's excavations.*

suggested that the deposit, including in the area where it was removed by construction work, contained only Early Acheulean lithics (Pollarolo *et al.* 2010). Geoarchaeological research conducted as part of the study indicated the artefacts at the marketplace, preserved in a buried clast[1]-supported 'pavement', are in secondary context (Pollarolo *et al.* 2010). A landscape-scale model for the formation of the 'pavement' was presented based on observations and sampling in Locations 1 and 2, near the edge of the marketplace (Fig. 2) (Pollarolo *et al.* 2010).

Subsequent observations at Maropeng from both construction cuttings and expanded archaeological excavations revealed that this artefact-bearing horizon[2] (ABH), is present across a large area of the property, rather than being restricted to the area around the marketplace, and that there is notable spatial variation in its properties. This variability could affect the archaeological content of the ABH across the landscape in multiple ways, including: artefact density, the representation of different artefact size classes, and the preservation and integrity of assemblages at specific locations. All these factors influence the usefulness of lithic assemblages for technological interpretation like that presented in Moll (2017) as the removal of some artefact types (like small flaking debris), the abrasion of artefacts (potentially removing features like flake scars), and the sample size (controlled by artefact density) may reduce the amount of information an analyst could recover.

Subsurface gravel pavements, often referred to as 'stone-lines', containing ESA and/or Middle Stone Age (MSA) lithics are fairly common in Central Africa (see Mercador *et al.* 2002, and references therein). Interpretations of the formation of these horizons vary, and include differing contributions by geogenic, pedogenic (soil formation, leading to the development of distinct horizons), and even anthropogenic processes. 'Stone-lines' have also been reported in many parts of southern Africa, including in South Africa, Eswatini, and Zimbabwe (e.g. Stocking 1978; Price Williams *et al.* 1982; Watson *et al.* 1984; Shakesby & Whitlow 1991; Will *et al.* 2024). Lithics found within different 'stone-lines' have been variously associated with the ESA, MSA, and Later Stone Age (LSA). These horizons have typically been considered to be buried lag deposits, rather than being pedogenic in origin (i.e. formed by subsurface movement of clasts). To date, there have been no detailed geoarchaeological studies of these buried horizons published in southern Africa, resulting in a limited understanding of how artefacts have accumulated and have been impacted by post-depositional processes at these locations.

Geoarchaeological studies of Oldowan and Early Acheulean occurrences in South Africa have focused on cave contexts or relatively localised open-air deposits, with many studies of the latter associated with alluvial formation processes (e.g. Matmon *et al.* 2012; Stratford *et al.* 2012; Stratford *et al.* 2014; Goldberg *et al.* 2015; Toffolo *et al.* 2019; Lotter 2020; Goldberg *et al.* 2023). There is a general research bias towards cave and rock shelter sites across the entire South African Stone Age record, but a variety of open-air contexts have been investigated by geoarchaeologists utilising a range of approaches and methods to address different research questions (e.g. Butzer 1974, 1988; Lotter *et al.* 2016; Lukich *et al.* 2020; Herries *et al.* 2022; Wroth *et al.* 2022). However, most of these studies have focused on relatively small areas, where artefacts are concentrated due to human behaviour, favourable preservation conditions, or post-depositional movement. Landscape-scale studies of the accumulation and post-depositional modification of assemblages (e.g. Kandel *et al.* 2003; Oestmo *et al.* 2014; Phillips *et al.* 2023) are rare by comparison.

Maropeng offers a rare opportunity to understand patterns in site formation processes and (potentially) Early Acheulean hominin behaviour across a landscape that has a wealth of complementary fossil data derived from caves in the area. Therefore, a new geoarchaeological research project – the results of which are presented here – was conducted with three basic aims: 1) to clarify the spatial distribution of the ABH across the Maropeng landscape; 2) to determine whether the site formation model proposed for the marketplace can be used to understand the context of archaeological assemblages excavated from different parts of Maropeng; and 3) to use the higher resolution spatial and fabric data collected from the ABH excavation in the M2 site to develop a more detailed understanding of the formation of the ABH at this location, as a representative example of the ABH in general, and clarify the potential impacts of site formation processes on the lithic assemblage recovered.

SITE BACKGROUND

GEOLOGY

Maropeng is located within a geologically complex part of the Transvaal Basin (Fig. 1). The >2.4 Ga Malmani dolomites (in which the karstic cave sites of the CoH formed [Martini *et al.* 2003]) are overlain unconformably by (in stratigraphic order) the ~2.4 to ~2.2 Ga Rooihoogte, followed by the Timeball Hill and Hekpoort Formations of the Lower Pretoria Group (Eriksson *et al.* 1993; Obbes 2000; Catuneanu & Eriksson 2002). The Rooihoogte Formation comprises conglomerates of the Bevets Member, an unnamed lower shale unit, and the overlying quartzites of the Polo Ground Member. The Timeball Hill Formation contains upper and lower shale members that sandwich the quartzites of the Klapperkop Member. The overlying Hekpoort Formation is volcanic in origin, mainly comprising extrusive andesites and dolerites. Dolerite has been reported as the bedrock in several excavations at Maropeng, and there are also several outcrops across the Maropeng landscape (Pollarolo *et al.* 2010). The dolerite likely represents various sills that formed during the igneous intrusions into the Pretoria Group associated with the formation of the Bushveld Complex (Cawthorn *et al.* 1981; Cawthorn 2015). The presence of so many different lithologies in the area has implications for landscape geomorphic evolution, vegetation distribution, sedimentology and pedogenic processes, hydrology, and hominin landscape utilisation.

Quartzite is the dominant raw material utilised in the Maropeng lithic assemblages (Pollarolo *et al.* 2010; Moll 2017). The presence of quartzites in multiple formations outcropping within the immediate vicinity means that access to raw material at Maropeng during the Early Acheulean would have been comparatively easy (Tasker 2020). However, high local lithological variability of the quartzites influences their knapping quality, and some raw material may have been sourced from as far as 2.8 km from Maropeng (Tasker 2020). This interplay between raw material quality and availability may have influenced reduction strategies and intensities practiced by hominins on the Maropeng landscape (Tasker 2020).

TOPOGRAPHY

Topography plays a vital role in the formation and preservation of a deposit (Goldberg & MacPhail 2006: 43). It impacts the mode and energy of sediment transport and deposition, how widely a deposit is distributed, and its morphology. It also affects the type and energy of erosional processes, influencing the likelihood of modification of a deposit through the removal of some sediment size classes, or the erosion of all or part of a deposit. This is of particular significance when considering deposition and erosion at the landscape scale, where these factors may vary due to local topographic variation. The geology at Maropeng significantly affects the topography, with ridges of quartzites and shales elevated above the undulating lower elevation areas dominated by dolerites.

The most prominent geomorphic feature in the immediate vicinity of Maropeng is a large quartzite outcrop with a maximum elevation of 1675 m, which forms a ridge to the east of the marketplace (Pollarolo *et al.* 2010: fig. 4). The ridge slopes gently down westward towards the Maropeng property. To the northwest of the property, a lower hill rises up to an elevation of ~1655 m. The marketplace and museum (Fig. 2) lie on an area of relatively flat ground 150–200 m across (north to south) with an elevation of ~1638–1640 m, which stretches roughly east–west between these two landforms. The landscape descends to the north and south, forming a saddle. The southern slope is comparatively gentle, flattening at the R400 road, which marks the southern boundary of the property. The northern slope descends steeply north of the Tumulus building, which houses the museum (Fig. 2). This has implications for the deposition and erosion of deposits on these slopes, with these processes likely to be of far higher energy on the steeper parts of the northern slope than elsewhere.

ARCHAEOLOGY

Research into the subsurface archaeology of Maropeng began following the discovery of lithic artefacts during construction of the marketplace (Pollarolo *et al.* 2010) (Fig. 2). Typologically diagnostic artefacts collected from the construction dump site and a smaller assemblage excavated from the *in situ* ABH at M1 (previously called Location 2) (Fig. 2), were analysed by Pollarolo *et al.* (2010), who suggested that the ABH is dominated by Early Acheulean technology. This was determined based on several factors. The presence of large cutting tools (LCTs) is diagnostic of Acheulean technology, and comparison of the Maropeng LCTs to those recovered from known Early Acheulean sites like Sterkfontein and Rietputs 15 (see Kuman 1998; Kuman & Gibbon 2018) revealed significant similarities (Pollarolo *et al.* 2010). The absence of prepared cores and more refined LCTs, both associated with later stages of the Acheulean, further support the attribution of the Maropeng assemblages to the Early Acheulean (Pollarolo *et al.* 2010).

Subsequent excavations of the ABH, led by Stratford, began in 2011. This included the expansion of Location 2 (now called M1) and the opening of new excavations: M2, M3, M4, and South Pit (Fig. 2). The objective of the expanded excavations was to recover a larger assemblage from the *in situ* ABH for technological and spatial analysis, and to test hypotheses posed by Pollarolo *et al.* (2010) regarding the morphology of ABH around the marketplace, which was proposed to represent a local depocentre. The technological analysis of this assemblage, which further demonstrates a dominant Early Acheulean component within the ABH (Moll 2017), and compares the assemblage to relevant Early Acheulean assemblages, will be presented elsewhere (Moll *et al.* in prep).

GEOARCHAEOLOGY

The stratigraphy at M1 (Fig. 2) was described briefly by Pollarolo *et al.* (2010). There, the decayed dolerite bedrock is overlain by compact red clay-rich sediment. The ABH overlies the clay-rich sediments and, in places, directly overlies decayed dolerite. The ABH is (on average) 0.3 m thick, buried 0.7 m below the surface, and composed primarily of poorly sorted rounded to semi-rounded quartzite clasts. The ABH is covered by a layer of clay-rich sediment similar to that beneath it, which is then capped by thin reddish-brown 'humitic' soil (Pollarolo *et al.* 2010: 6).

The existing site formation hypothesis for this area of Maropeng proposes that the artefactual material accumulated through colluvial processes into a natural palaeo-depression (depocentre) in the landscape (around the current marketplace) (Pollarolo *et al.* 2010: fig. 4). This colluvium would have included natural and artefactual clasts, along with finer sediment, which was subsequently winnowed, resulting in the formation of a pavement-like ABH. The gentle topography (Pollarolo *et al.* 2010: fig. 4) suggests that both the deposition and deflation would have involved relatively low energy depositional and winnowing processes. The sediment overlying the ABH also appeared to be colluvial, with the presence of a 'humitic' horizon indicating at least some pedogenesis (Pollarolo *et al.* 2010). The quartzite ridge (~200 m east of the marketplace) was proposed to be a dominant source of the clastic material contributing to the ABH (Pollarolo *et al.* 2010: fig. 4). The topography of the dolerite bedrock was argued to have effectively constrained the ABH to the general area of the marketplace (Pollarolo *et al.* 2010).

Observations subsequent to Pollarolo's interpretations, which derive from limited exposures (Fig. 2) near the marketplace, warrant expanded investigation of property-wide formation processes. Spatially broader investigation will allow a more comprehensive and nuanced interpretation of the formation of the ABH, and allow a more subtle understanding of hominin utilisation of the Maropeng landscape. While it is important to understand the general formation processes and the factors influencing the distribution of the ABH, there is also a need to apply more detailed analysis of the context of the assemblage excavated from M2 in order to provide high resolution site formation perspectives that can be considered representative of the broader, landscape-scale patterns exemplified by the more distal ABH exposures. Improving interpretations at both landscape and site scales requires the application of a multi-scale approach, and complementary methods.

METHODOLOGY

The following methodology was applied at Maropeng to address the aims of this study by determining the extent of the ABH across the property, clarifying depositional and post-depositional processes involved in its formation, identifying any spatial differences in these processes across the landscape with reference to the local geomorphological context, and providing specific site-scale insight into the formation of the ABH in the M2 excavation.

EXCAVATION AND SPATIAL RECORDING

Test pits, a geotrench and a full excavation (M2) were excavated across the property. They were distributed to provide maximum spatial information on the extent of the ABH. Data were obtained from sedimentary profiles exposed in ten locations (Fig. 2), including seven test pits, a geotrench excavated into a cutting, the walls of a fire pit dug by construction workers during the building of the accommodation blocks at Hominid House, and the M2 excavation. These excavations and exposures were named based on nearby outdoor museum activity or exhibit areas, buildings, or some aspect of the specific location. They include the Amphitheatre Geotrench (AGT), Africa Forms Test Pit (AFTP), Boulder Test Pit (BTP), Empty Test Pit (ETP), Hominid House Fire Pit (HHFP), Hominid House Test Pit (HHTP), Hotel Test Pit (HTP), Molehill Test Pit (MHTP), and Triassic Park Test Pit (TPTP) (Fig. 2).

Excavation of the test pits and geotrench was carried out using the following technique: 1 m × 1 m pits (the geotrench was 0.5 m wide) were dug using picks and spades. Once the upper surface of the ABH was exposed in each test pit, it was excavated by trowel. The sediment removed from the pits at depths deeper than 0.2 m was dry sieved with a 2 mm sieve. Any artefacts recovered *in situ* or from sieving both within and above the ABH were kept and the depth below surface recorded. The M2 excavation covered 4 m^2 and was conducted at greater stratigraphic sensitivity than the test pit excavations. High resolution spatial data were collected for both artefacts >20 mm and some natural clasts (see greater detail below), and sediment removed from the excavation was dry sieved with a 2 mm mesh.

In order to compare the relationship between past topography and the ABH at the different sample locations, it was necessary to determine the elevations of: (a) the current surface; (b) the top of the ABH (the depth of the deposit); and (c) the base of the ABH at each location. This allowed the comparison of ABH depth and thickness across the property. Surface elevation was obtained using a Trimble R6 Differential GPS (DGPS) unit calibrated to the main site datum (25°58′05.16396″S; 27°39′44.90844″E; 1642 m above mean sea level). The elevation of the top and base of the ABH were determined by measuring their depth below the surface using a tape measure, with those values subtracted from the calibrated DGPS elevation of the surface at the sample location.

IN SITU SEDIMENT DESCRIPTION AND SAMPLING

Facies were defined through macroscopic documentation of exposed sediments in test pit profiles based on standard sedimentary variables like colour, texture, sorting, grading, and structure. Sediment samples were collected from the ABH and facies above it, and were prepared for laboratory analysis of microscopic and granulometric attributes.

The following sedimentary variables were also documented *in situ* as they are particularly useful for characterising the formation of clast-rich deposits:

1. Clast size data can provide an idea of the extent and nature of the erosional and/or depositional processes involved in the formation and modification of a deposit (Petraglia & Potts 1994; Pye 1994; Selby 1994; Rapp & Hill 1998: 39–40). Clast size was quantified by measuring the maximum observable length of natural clasts and artefacts visible in the exposed profiles of the test pits. Artefactual clasts yielded from excavation were measured using callipers.
2. Clast shape (assessed as angularity) is influenced by the degree to which a clast has been moved by natural processes, but also by the material properties of the rock, with the latter impacting abrasion during movement and subsequent weathering (Pye 1994; Rapp & Hill 1998: 40–43). Angularity was determined through visual examination of clasts in the profiles of the test pits and quantified using standard shape categories (Mazzullo & Graham 1988). To control for the effects of lithology, only quartzite clasts were analysed. There is no indication that the quartzite decays *in situ*, unlike the dolerite, making it a good comparative proxy for the transport distance of clasts at Maropeng. The dominant quartzite angularity type for each excavation was recorded.
3. Deposit fabric (the three-dimensional organisation of clasts within a deposit) is used to identify the direction and intensity of water or colluvial flow involved in site formation (Bluck 1987; Bertran & Texier 1995; Evans 2000; Lenoble & Bertran 2004). Fabric analysis can also be a helpful indicator of post-depositional disturbance through bioturbation (Goldberg & MacPhail 2006: 24), which is of particular relevance at Maropeng given the relatively shallow depth of the deposit and active pedogenic processes. Fabric data were obtained from the test pits by determining the orientation and dip of clasts exposed in the walls. Given that orientation could only be recorded to the nearest main cardinal point (north, east, south, west) in these conditions (with a limited understanding of the three-dimensional shape and position of the clasts), these data can only be used to estimate very broad trends. Interpreting the magnitude of the dip of clasts is not hampered to the same degree by recording these data from the profiles. Consequently, these observations are considered more informative than the orientation for understanding depositional and post-depositional processes at Maropeng in this specific case, as they reflect the deposit fabric more accurately. Only flat-bottomed clasts were considered in the fabric analysis. The dip angle of each clast relative to horizontal was recorded to the nearest 5° from photographs calibrated using a spirit level, while the orientation was estimated from the apparent dip direction of elongated clasts.

The excavation of the dense ABH in M2 provided an opportunity to conduct fabric analysis as part of a piece-plotted spatial documentation approach. Understanding the fabric in this location provides a means to assess the depositional and post-depositional context of the M2 lithic assemblages at higher resolution than was possible from test pits, and assess the implications for the integrity of this assemblage with greater sensitivity. High-resolution three-dimensional spatial data were collected using a Nikon Nivo 5C total station following McPherron (2005) and Stratford (2011). The central points of elongated (length at least 1.6 times the width) artefacts >20 mm and natural pieces >50 mm, and the opposing ends of their axes of maximum length (for artefacts <50 mm) and maximum length and width (for artefacts >50 mm) were plotted from the surface beneath each piece. Surveyed points were used to calculate the orientation and dip angles of each piece using the approach modified by Stratford (2011) from McPherron (2005). The approach and code of McPherron (2018) were used to visualise the results in a ternary Benn diagram (Benn 1994), aiding meaningful comparison with published datasets from archaeological and/or geological contexts. The total station spatial data (including central points for the bottoms of all equant artefacts >20 mm and naturals >50 mm) were also used to document the lateral and vertical distribution of various clast and artefact types (e.g. elongated vs. equant pieces; core vs. flake) within the deposit.

Bulk sediment sampling was conducted to augment inter-facies comparisons by determining the microscopic and granulometric properties of the different facies identified in each test pit. A single bulk sediment sample (~150–200 g) was taken from the middle of each facies within each of the test pits to avoid contamination from any mixing between facies near the transitions.

LABORATORY SEDIMENT AND ARTEFACT ANALYSES

The following analyses were conducted in the laboratory using samples taken from the sedimentary profiles of the excavations (see above) or the artefacts yielded from the excavation of the ABH across Maropeng:

1. Analysis of artefact abrasion can be used to determine if an artefact has been moved significantly by natural processes, with heavier abrasion associated with longer transport distances (Petraglia & Potts 1994; Shea 1999). As discussed previously, different lithologies undergo differing degrees of abrasion during transport and diagenesis. For consistency with the analysis of natural clasts, only quartzite artefacts were analysed. Following an adapted version of the technique applied by Shea (1999), each quartzite artefact from the test pits and M2 was classified as belonging to one of four abrasion classes (none, slight, intermediate, or heavy) after macroscopic visual analysis of two properties – surface texture and edge condition. Lithics assigned to 'none' had a matte surface texture and no significant edge damage. Those attributed to 'slight' had a matte surface texture and micro-fracturing on their edges, but no rounding. 'Intermediate' artefacts had a smoothed matte surface texture and both rounded and sharp edges. Finally, 'heavy' included those with smooth surface texture and rounded edges.
2. Sediment particle size data can provide valuable evidence of the depositional environment and the contributing components to

TABLE 1. *Macroscopic sedimentological properties of Facies 2 (including the ABH) at the test pit locations across Maropeng. The categories for clast abrasion/angularity are: angular (A), sub-angular (SA), sub-rounded (SR) and rounded (R). Note that only quartzite natural clasts and artefacts were analysed for abrasion.*

	Description	Contacts		Clast abrasion (angularity)		Clast size range (mm)		Particle sphericity %	
		Upper	Lower	Natural	Artefact	Natural	Artefact	Low	High
HHFP	Clast-supported with loamy fine sand matrix. Quartzite and quartz clasts spread diffusely throughout the pisoliths, but most concentrated in the upper part. The ABH is 18 cm thick.	Sharp	Diffuse	R		2–80		50	50
HHTP	Clast-supported and dominated by pisoliths with loamy fine sand matrix. Some small quartzite and quartz clasts visible throughout, but mainly in the upper few centimetres. The ABH is 20 cm thick.	Sharp	Sharp	SR	R	2–20	41–93	53.3	46.7
AFTP	Matrix-supported loamy fine sand with no pisoliths. Quartzite and quartz clasts are spread diffusely within the matrix. Thickest in the south of the excavation, but thins towards the north, and eventually terminates against a dolerite clast. The ABH is 5–10 cm thick.	Sharp	Sharp	R	SA	6–80	22–141.5	50	50
TPTP	Three distinct strata with loamy fine sand matrix. Lowest: tightly packed quartzite and quartz clasts with no pisoliths. Middle: massive, matrix-supported with pisoliths but few other clasts. Upper: clast-supported quartzite and quartz clasts with very few pisoliths. The ABH is 36–45 cm thick.	Sharp	Sharp	R	SA/SR	4–120	20.5–111.5	57.1	42.9
AGT	Clast-supported with loamy fine sand matrix. Mainly composed of pisoliths. Quartzite and quartz clasts present throughout, but most are tightly packed in the top few centimetres. The ABH is 15 cm thick.	Sharp	Sharp	A	SA	2–135	45–118	62.5	37.5
MHTP	Clast-supported with loamy fine sand matrix. Dominated by pisoliths. Quartzite and quartz clasts are spread diffusely throughout but mostly concentrated in the top few centimetres. The ABH is 30 cm thick.	Diffuse	Sharp	A/SA	A/SA	3–150	23–83	73.1	26.9
ETP	Clast-supported pisoliths and sandy loam matrix. No clasts other than the pisoliths and one sub-rounded quartzite clast are present. The ABH is absent.	Diffuse	Sharp			2–14	–	67.5	32.5
BTP	Clast-supported loamy fine sand matrix. Quartzite and quartz clasts present throughout the pisoliths, but mostly in the top five centimetres. The ABH is 25 cm thick.	Diffuse	Sharp	A/SA	SA/SR	2–119	9–74.5	72.7	27.3

a deposit (Stein 1985; Pye 1994). Granulometry was conducted using the Malvern Mastersizer 3000 laser granulometer on samples which had undergone heating at 590°C for eight hours to burn off any organic matter.

3. Sediment particle shape analysis can help to identify different processes which transported material into a site while also indicating the distance of transport (Stein 1985; Pye 1994). Particle shape was determined by examining sand-sized grains in the sediment samples under an optical microscope (an Olympus BX41) using direct lighting at 40x magnification. A representative subsample of grains from each sample was classified and the proportion of each of the categories in the subsample noted. Quartz grains, which make up almost all the particles in this size range in the samples, seldom become rounded during transport by fluvial or colluvial processes (Gomez *et al.* 1988). Therefore, the sphericity of grains (Powers 1953) is expected to be a better indicator of transport in this context than their angularity/roundedness. Generally speaking, the further sediment has been transported, the more spherical the quartz particles within it will be (Stein 1985; Pye 1994).

RESULTS

STRATIGRAPHY, FACIES IDENTIFICATION AND DISTRIBUTION

Four facies were identified in the same stratigraphic order consistently across the landscape, with only a few exceptions.

The basal Facies 1 is a massive highly compacted matrix-supported yellowish-red or yellowish-brown clast-free sediment. The average thickness of Facies 1 is unknown as none of the excavations or test pits reached bedrock except AFTP, and excavation seldom continued more than a few centimetres below Facies 2. The contact between Facies 1 and 2 is sharp at all locations except HHFP.

Facies 2 is the most complex and variable of the identified facies (Table 1). It ranges between 5 and 45 cm in thickness and includes two clast-supported sub-facies, which have undergone varying degrees of mixing, and some patches and lenses of matrix-supported sediment. The lower sub-facies is dominated by small (<25 mm) rounded to sub-rounded 'pellets' that have yellowish or reddish exteriors and black interiors. Some have indurated red clay coatings. Several rounded nodules of 'pellets' and red clay matrix were recovered from BTP – these ranged from ~4 cm to ~7 cm in length. The pellets were previously interpreted as decayed dolerite (Morrissey 2015), but appear more likely to be pedogenic concretions, specifically siliceous and iron-rich pisoliths, which are frequently associated with the *in situ* weathering of mafic rock types and laterite formation (Bourman 1993; Taylor & Eggleton 2008; Lascelles 2016; Sarkar *et al.* 2020). The upper sub-facies is dominated by poorly-sorted quartzite, quartz, and dolerite clasts and is what we have termed the ABH. The frequency of mixing in most cases necessitates that these two sub-facies be considered together rather than as wholly distinct facies/deposits. The properties of Facies 2, and the variation therein (Table 1), are considered in

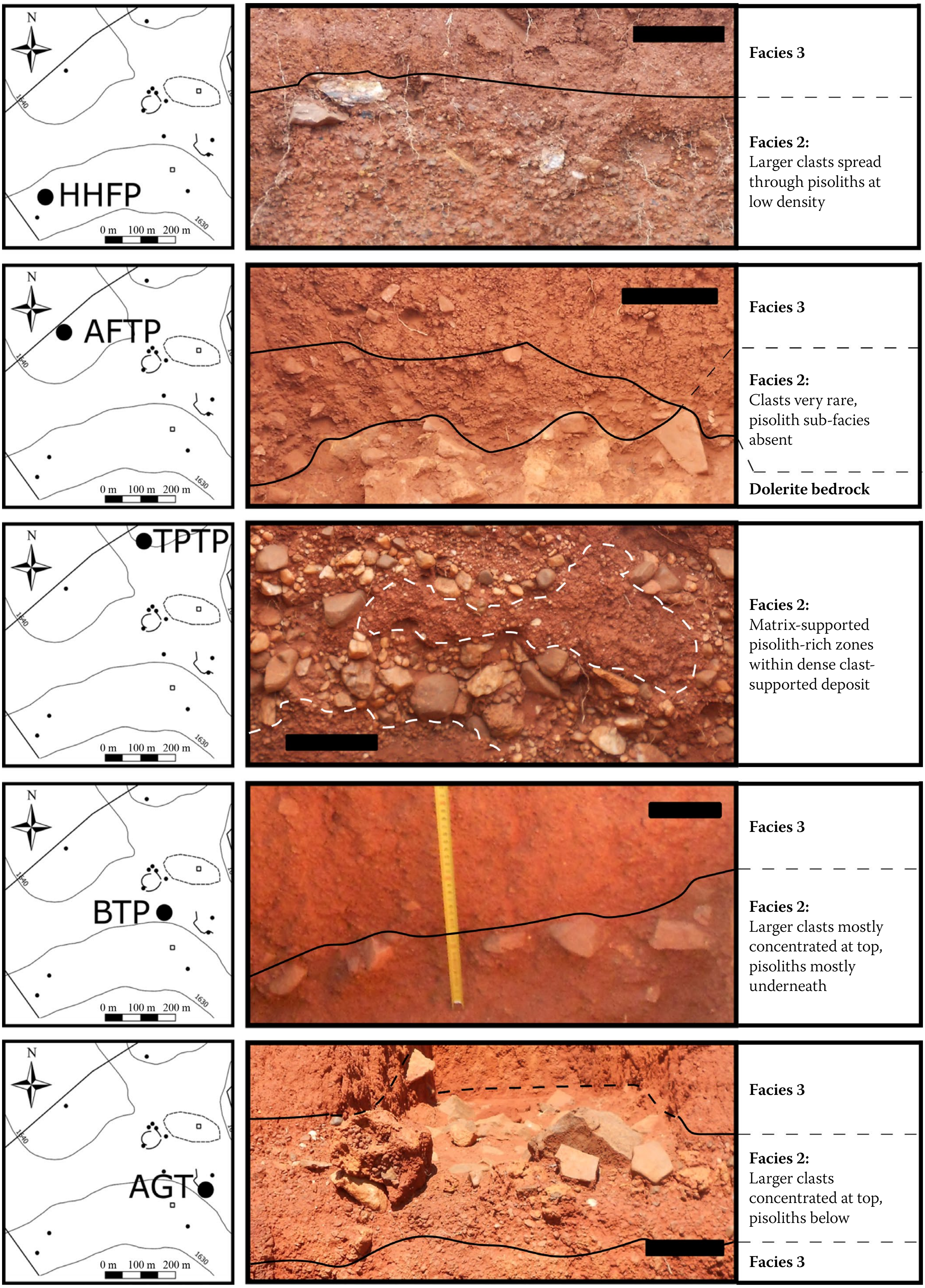

FIG. 3. *Photographic examples of the variation in Facies 2 (including the ABH and pisolith sub-facies) at different test pit locations at Maropeng. The scale bar in each photograph is 10 cm in length.*

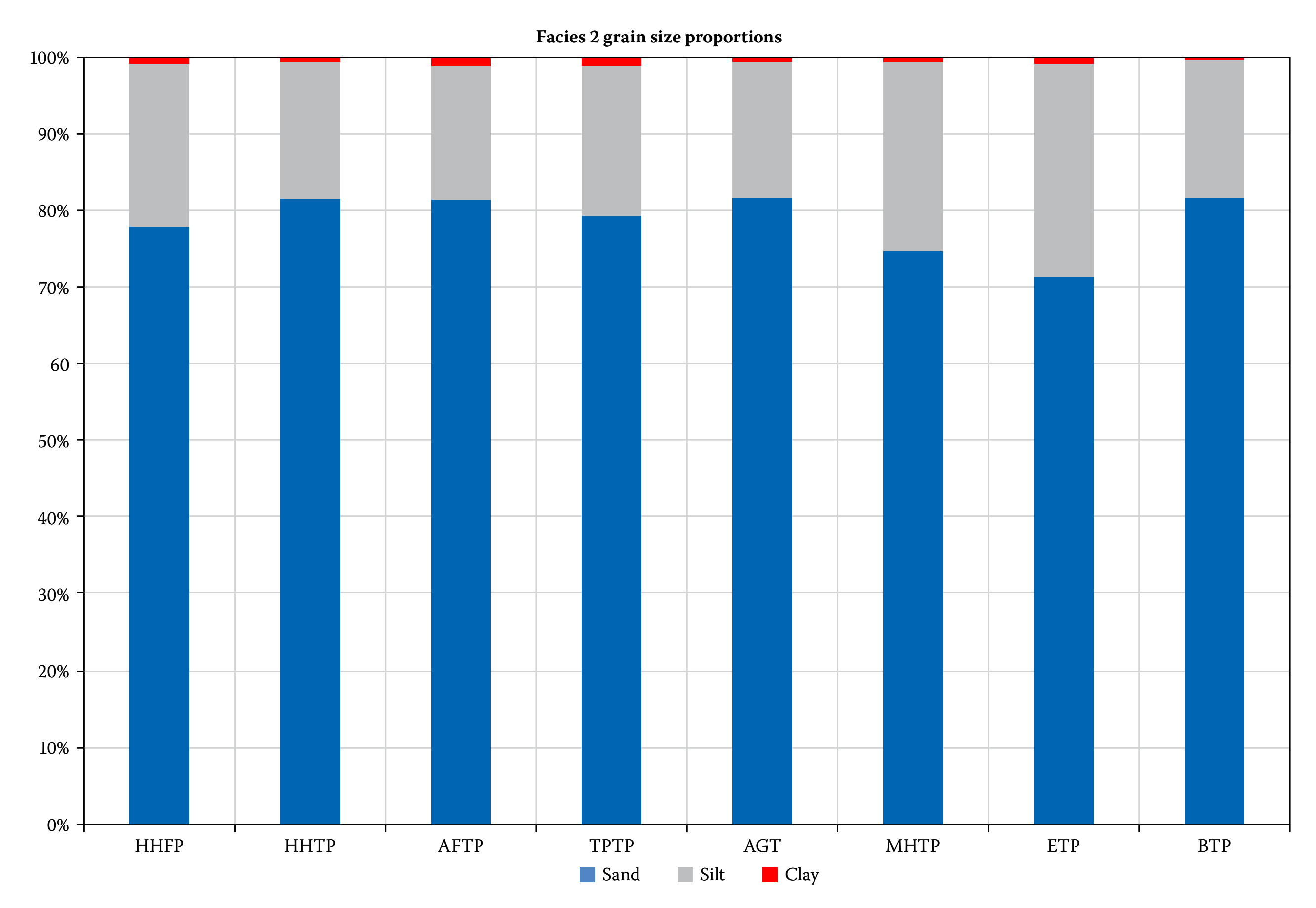

FIG. 4. *The proportions of sand, silt, and clay in the samples collected from Facies 2 across the study area.*

more detail below. The upper contact with Facies 3 is mostly sharp, but is diffuse at MHTP, ETP, and BTP.

Facies 3 is between 10 and 45 cm thick and is matrix-supported reddish loamy sand or sandy loam with few clasts. It is massive in most cases, but sometimes columnar in structure. Both vertical cracks and small roots are common. This facies has a diffuse contact with the overlying Facies 4, which is a 17 to 55 cm thick, columnar, matrix-supported, reddish-brown loamy sand with few clasts. Vertical cracks are present throughout, as are small roots. These two facies appear to correspond to A and O soil horizons respectively. Four of the test pits – HHTP, AFTP, TPTP and BTP – yielded occasional isolated Middle and/or Later Stone Age lithics from varying depths within Facies 3 and 4. These artefacts were almost exclusively produced on quartz and include small (<50 mm) cores and flakes.

Three locations differ from the general sequence described above (Fig. 2). The ABH (upper sub-facies of Facies 2) is absent at ETP, but all other facies, including the pisoliths rich lower sub-facies of Facies 2 are present. At AFTP, Facies 1 is absent, and Facies 2 lies directly on decayed dolerite. Inversely to ETP, the ABH is present, but very limited in thickness, clast density, and extent across the test pit, but no pisoliths were found. HTP differs entirely, comprising slate bedrock overlain by a clast-supported sandy loam rich in angular slate clasts with none of the clast types and artefacts that characterise the ABH.

FACIES 2 IN THE TEST PITS, GEOTRENCH AND FIRE PIT

GENERAL CHARACTERISTICS

There is considerable variation in the density of artefacts and natural quartzite, dolerite and quartz clasts, while the pisoliths remain very common in all locations except AFTP, where they are entirely absent (Table 1). The degree of mixing between quartz and quartzite clasts (the upper sub-facies) and pisoliths (the lower sub-facies) ranges from the clasts forming a fairly clearly defined horizon on top of the pisoliths through to the clasts being contained entirely within the pisolith horizon (Fig. 3, Table 1).

PARTICLE AND CLAST SIZE AND SHAPE

The ABH has a lower proportion of spherical sand-sized particles on the eastern side of Maropeng than it does to the west. TPTP has a significantly lower proportion of spherical particles than AFTP (west), HHTP and HHFP (both south-west). Particle size showed little variation across the landscape (Fig. 4), with the proportions of sand, silt and clay consistent with sandy loam at all sampled locations. Sand is the dominant size class, ranging from 71.6% (ETP) up to 81.8% (MHTP). Silt is also a significant component, with a minimum of 17.3% (AFTP) and a maximum of 27.6% (ETP). Clay is very limited: as little as 0.3% at BTP, and only 1.1% at its highest (TPTP). The particle size distributions were all poorly sorted and either bimodal or polymodal.

The largest natural clasts within the ABH at locations in the west and south-west of Maropeng are considerably smaller than those at the rest of the locations (Table 1). At HHTP and AFTP, artefacts were found which were significantly larger than the largest natural clasts. There is a clear difference between the eastern side of Maropeng, where natural quartzite clasts are angular, and the western side, where they are rounded due to abrasion (Table 1). Quartzite artefacts yielded from the eastern excavations are generally less abraded, while those from the western excavations tend to be more abraded (Fig. 5). TPTP, in the north-west, has a less

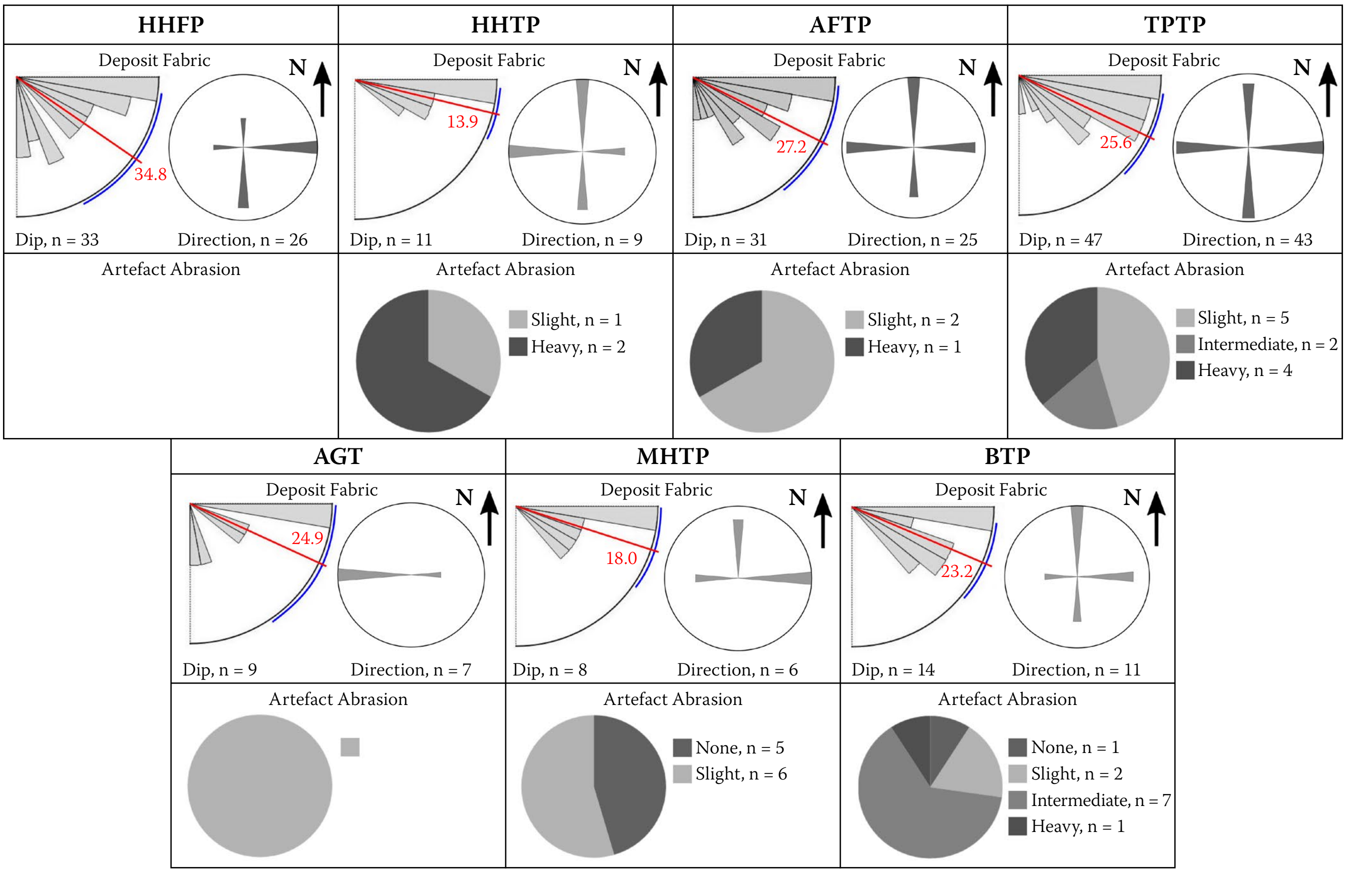

FIG. 5. *The results of the analysis of deposit fabric and artefact abrasion for the ABH at the test pit locations across Maropeng. Note that the directions are limited to the four main cardinal points due to the limitations of recording these data from the profiles. The red lines and text indicate the mean dip for each location, and the blue lines show the standard deviation of the dip.*

abraded assemblage than those recovered from AFTP (west) and HHTP (south-west).

DEPOSIT FABRIC AND THICKNESS

Clasts in the ABH do not have clear preferred orientations in most of the excavations. Most clasts across Maropeng have a dip from the horizontal that falls within the range of 0° to 10°. However, some clasts at all locations (but more so at some than others) have considerably greater dips – up to 90° in some locations (Fig. 5).

The depth below surface level and the thickness of the ABH varied with no discernible spatial patterning (Table 2). It was shallowest at HHFP (0.42 m below the surface) and deepest at MHTP (1.10 m), and was less than 0.5 m deep at only two locations (HHFP and AFTP). The ABH was only ~5–10 cm thick at AFTP, and ranged from 15 to 45 cm at the other locations.

FACIES 2 IN THE M2 EXCAVATION

SEDIMENTARY DESCRIPTION

As in the test locations, the ABH (part of Facies 2) at M2 is overlain conformably by Facies 3 and 4. These upper units (~50 cm in maximum combined thickness) do not differ appreciably from their equivalents at the other logged locations. Facies 2 has the same broad general properties as recorded at the test pits. It comprises two layers – the upper ABH and a lower layer dominated by pisoliths. The ABH is a clast-supported layer, but occasional pockets of loamy fine sand were found to disrupt the relative homogeneity of clast density (Fig. 6A). The vertical extent of the layer varies considerably, but it is a little over 10 cm thick at its thickest. The clasts are a poorly sorted mix of quartzite, dolerite and quartz and include both artefacts and natural pieces. They range in size from a few millimetres to 226 mm

TABLE 2. *The coordinates, surface altitude and the depth of the ABH (if present) below surface level at each test pit location.*

	Coordinates	Surface altitude (masl)	ABH depth below surface (m)	ABH thickness (m)	Underlying surface altitude (masl)
HHFP	25°58′15.49″S, 27°39′32.55″E	Not measured	0.42	0.18	No data
HHTP	25°58′17.45″S, 27°39′31.33″E	1641.14	0.90	0.20	1640.04
AFTP	25°58′2.91″S, 27°39′34.26″E	1641.91	0.47–0.52	0.05	1641.34
TPTP	25°57′58.02″S, 27°39′42.49″E	1636.12	0.85	0.36	1634.91
AGT	25°58′11.22″S, 27°39′48.77″E	1642.46	1.05	0.15	1641.26
MHTP	25°58′14.83″S, 27°39′46.67″E	1638.16	1.10	0.30	1636.76
ETP	25°58′12.72″S, 27°39′45.11″E	1638.47	N/A	N/A	N/A
BTP	25°58′9.40″S, 27°39′44.23″E	1640.65	1.05	0.25	1639.35

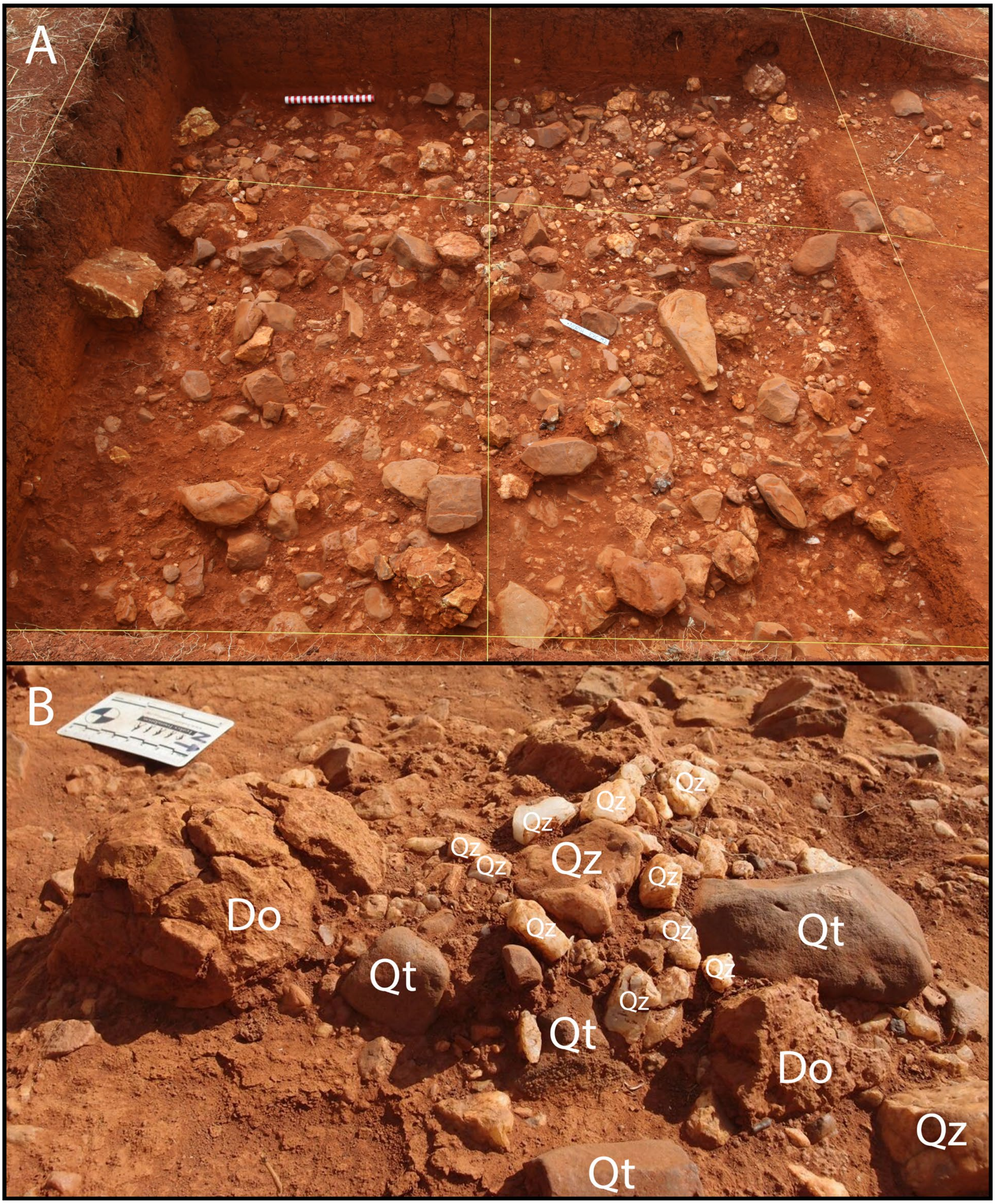

FIG. 6. *A) The ABH exposed in the M2 excavation. Note the pockets of matrix-supported sediment. The scale is in centimetres (30 cm in length). The white arrow points north. The two squares to the far right (partly visible in photograph) were not excavated further as they provided a protective baulk for the four fully excavated squares. B) In-situ shattering/breakage of dolerite (Do) and quartz (Qz) clasts within the ABH at the M2 excavation. Note the unaffected quartzite (Qt).*

in length. On average, the natural clasts range from sub-angular to sub-rounded. Pisoliths are also common in the ABH. In contrast, few larger clasts were observed in the pisolith horizon, although little of it was excavated.

In situ decay, exfoliation and shattering of dolerite clasts was commonly observed, as was the in-situ shattering/breakage of quartz (Fig. 6B). The size of the resulting pieces varied widely, and in some cases, it appeared that broken material had moved around within the deposit. This was also observed in some of the test pits excavated for this study, but no mention of it was made by Pollarolo *et al.* (2010) in their test pits and excavations.

SPATIAL DATA, ABRASION, AND FABRIC

The spatial data recorded during excavation suggest that there are no specific patterns in the lateral or vertical distributions of artefactual and natural clasts, equant and elongated clasts, and the different recorded abrasion states of quartzite artefacts (Fig. 7). All these clast classes are mixed throughout the deposit. In comparison

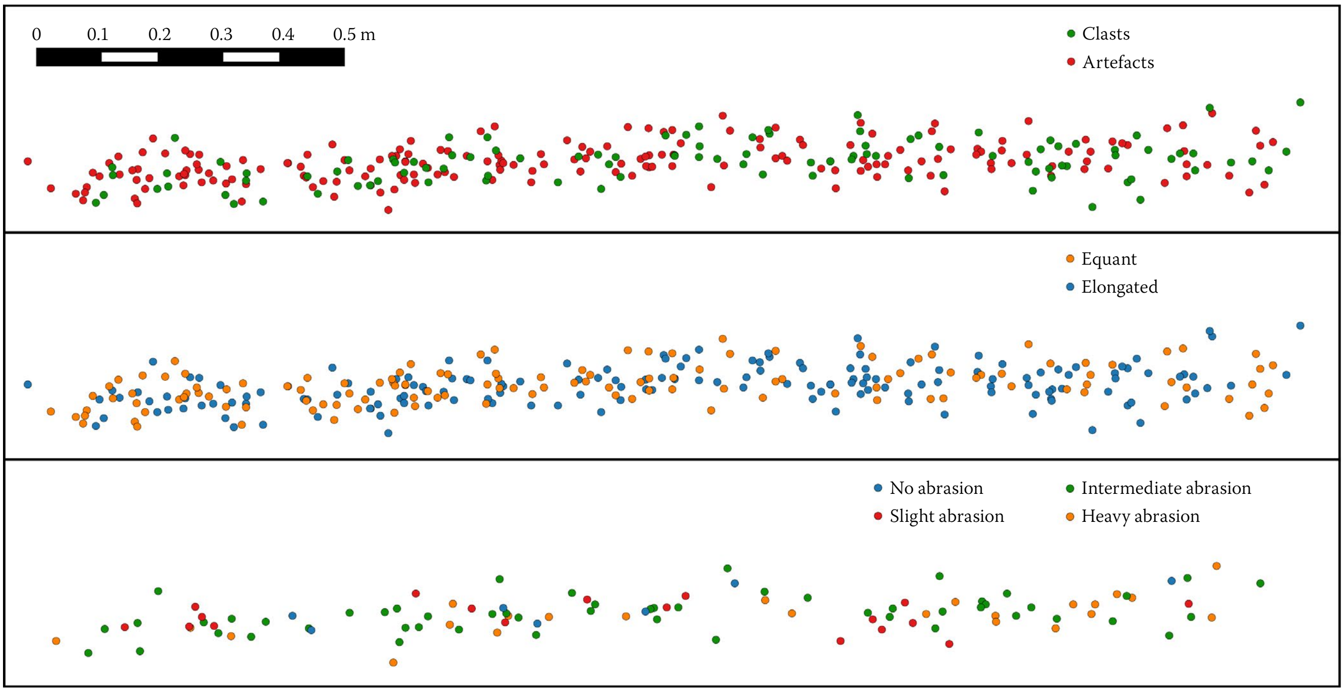

FIG. 7. *The vertical and lateral distributions of clast central plotted points within the ABH at M2. Top: natural clasts versus artefacts; Middle: equant versus elongated pieces (both natural and artefactual); Bottom: the quartzite artefacts and their abrasion classifications.*

to the test pits, artefacts were incorporated into the ABH at M2 at a relatively high density – 216 artefacts across 4 m^2. Quartzite artefacts with all four abrasion states – none, slight, intermediate, and heavy – were found (Fig. 8). Just over half of these 103 artefacts were classified as intermediate, while ~23% were heavily abraded. Slightly abraded and non-abraded pieces made up ~17% and ~7% of the quartzite artefacts, respectively.

The high-resolution three-dimensional spatial data obtained for the clasts in the ABH in M2 allow a more representative assessment of deposit fabric than those developed for the test pits (Fig. 9). Of the 190 elongated plotted clasts, 151 (79.47%) dipped at angles smaller than 30° from the horizontal. This includes 82 clasts (43.16%) that had dips gentler than 10°, and 44 clasts (23.16%) with dips between 10° and 20°. However, the clasts show no statistically significant preferred orientation. The Benn diagram plot for M2 records the same general pattern (Fig. 10). A strongly planar character accords with the lack of a preferred orientation, while the low to moderate isotropy is to be expected in an assemblage where few clasts were truly horizontal, but dip angles were typically gentle.

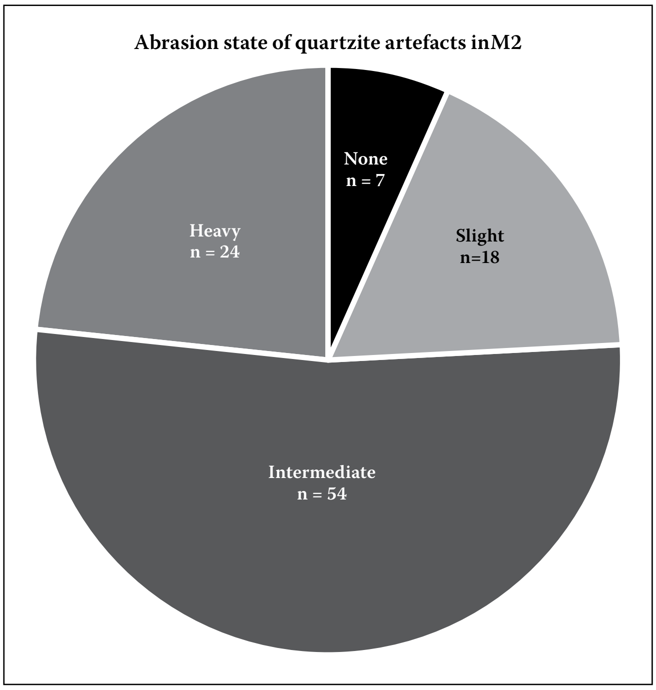

FIG. 8. *The proportions of the four abrasion classifications in the assemblage of 103 quartzite artefacts from M2 which were suitable for analysis.*

DISCUSSION

EXTENT OF THE ARTEFACT-BEARING HORIZON

A map of the inferred minimum area of the ABH (Fig. 11A) was created based on the locations of the excavations (and other exposures) where the ABH is known to be present. Using this inferred distribution, it was calculated that the ABH covers a minimum area of 191 200 m^2. It is, however, likely that the ABH extends beyond this area in some directions.

The ABH is absent in three excavations due to different local geomorphic and topographic characteristics. The area around Pollarolo *et al.*'s (2010) test pit is dominated by small dolerite outcrops that may have hindered the movement of sediment into this location. It is unclear if the pisolith-rich sub-facies occurs there. The absence of the ABH at ETP could be due to similar topographic obstacles, but the absence of exposed dolerite outcrops nearby means this cannot be confirmed. The ABH is present on all sides of ETP, in most cases at locations less than 100 m away. Removal of the ABH by water flow is unlikely because the lower Facies 2 pisolith-rich unit, which is present, would also have been eroded by a flow strong enough to erode the larger clasts, suggesting that the ABH was never deposited at ETP, although the specific reasons for this absence are not clear. The relative steepness of the slope beyond TPTP suggests that the preservation of the ABH would become far less likely due to the increased erosional processes on the slope. Thus, the complete absence of the ABH at HTP (Fig. 2), and the distinct deposits found there, are unsurprising,

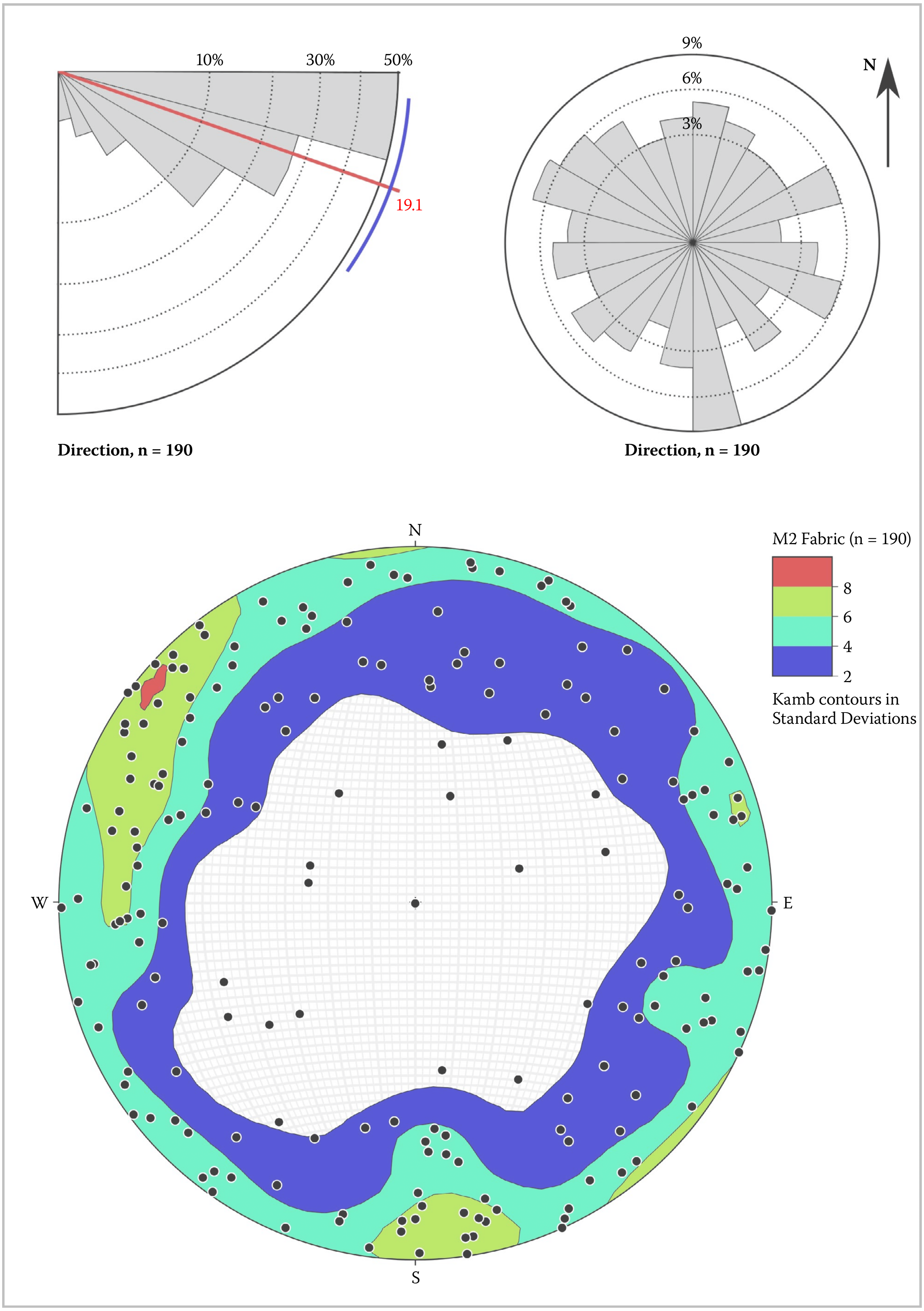

FIG. 9. *The dip and orientation of 190 elongated natural clasts and artefacts within the ABH at M2. Top: separate representations of these two factors; Bottom: both dip and orientation displayed in an equal area stereonet with Kamb contouring (3 sigma significance level). Note the predominance of shallower dip angles (clustering away from the centre of the projection) and the lack of a clear preferred orientation.*

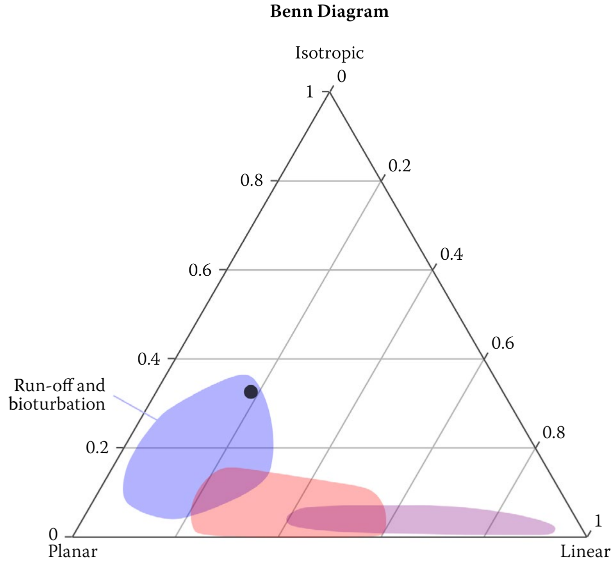

FIG. 10. *Benn diagram plot of the average three-dimensional orientation of clasts within the ABH at M2 (including lithics and natural clasts). The marked zones correspond to the values of deposits formed by run-off/slopewash on steeper (>20°) and shallower (<20°) slopes, and deposits which were bioturbated following deposition by run-off (Lenoble & Bertran 2004).*

representing a different lithological context associated with the decay and erosion of slate bedrock.

MODE AND ENVIRONMENT OF DEPOSITION

The spatial patterns in clast size and abrasion, and the sphericity of quartz grains (Table 1) suggest that the sediment in the ABH (the upper sub-facies of Facies 2) entered Maropeng from the east and flowed westward, with artefacts being entrained with the natural clasts and fines. Comparing the same data types from locations on the saddle and those on the slopes below the saddle (Table 1) indicates that the sediment flowed from the saddle and down the slopes on either side (Fig. 11B). Both the movement down from the ridge onto the top of the saddle and then down the sides of the saddle would have occurred gradually and through repeated events whenever there was sufficient precipitation for slopewash to occur. Reduction in clast frequency and size with increasing distance from the ridge and down the comparatively gentle southern slope of the saddle suggests a gradual loss of energy as the sediment travelled further from the ridge. In contrast, the very dense and thick ABH at TPTP is suggestive of greater flow energy down the relatively steeper northern slope, accumulating a greater number of clasts in this area.

The lack of clear preferred clast orientations in the ABH is unsurprising, as gentle slopes are generally low-energy environments where the development of a preferred orientation is unlikely (Mills 1983). The steep dip of some clasts is unusual given these slope angles (Fig. 5), and it most likely to be the result of post-depositional processes that are discussed in the following section.

The association between the ABH and the pisolith-dominated sub-facies of Facies 2 necessitates some discussion. The precise mechanisms by which individual pisoliths form and how they come to be concentrated in dense accumulations with limited matrix are debated (Bourman 1993; Taylor & Eggleton 2008; Thorne *et al.* 2014; Lascelles 2016). Pisolith formation is linked to weathering of mafic rocks and the resulting formation of iron-rich lateritic soils (Bourman 1993; Widdowson 2007). Formation of pisolith-rich soils occurs across wide geographical and climatological areas (Widdowson 2007) and there is considerable variety in the specific composition of pisolith cores and coatings, and how many layers make up the coatings (e.g. Taylor *et al.* 2008). Generally, pisoliths are considered to indicate soil formation under warm, humid climatological conditions and have been linked to significant seasonality (Bourman 1993; Widdowson 2007). Their initial formation often occurs subsurface in the vicinity of the water table where the core is coated by eluviated clay (as part of the decay of the bedrock) and iron minerals (Widdowson 2007) from the E soil horizon into the B soil horizon. Pisoliths may undergo multiple stages of growth (and weathering) at this depth, or at or near the landscape surface following erosion of the overlying soil (Bourman 1993; Taylor *et al.* 2008; Thorne *et al.* 2014). Reworking by fluvial and colluvial processes commonly occurs, as does the deflation of reworked or *in situ* sediment through the selective removal of sand, silt, and clay (Taylor & Eggleton 2008; Thorne *et al.* 2014; Lascelles 2016). Consequently, the presence of a pisolith-rich deposit is often indicative of multiple stages of landscape evolution (Taylor & Eggleton 2008; Thorne *et al.* 2014).

The pisolith-rich sub-facies at Maropeng could be explained by either the colluvial reworking of lateritic material from across the landscape, or by the deflation of *in situ* pisolith-bearing autochthonous soil through the selective removal of finer sediment. The possibility that a single location could have a mixture of both autochthonous and locally reworked pisoliths cannot be ruled out. The well-sorted rounded/sub-rounded pisoliths across Maropeng and the rounded aggregates of pisoliths and indurated clay matrix recovered from BTP suggest erosion and transport of much of this material (Bourman 1993; Taylor & Eggleton 2008). However, this process differed from the erosion and transport of the artefact-bearing clast-rich material from the higher elevation, quartzite-dominated areas. Most of the natural sediment in the ABH was eroded from the vicinity of the quartzite ridge and was initially transported down a relatively steep slope. As discussed above, laterite formation occurred in association with the lower-lying dolerites. Consequently, the colluvial reworking of the pisoliths would have taken place over shorter distances, from more local sources. The lack of larger clasts, and the location of the material sources on a gently sloping landscape indicate lower energy slopewash than that associated with the formation of the ABH. The larger aggregates at BTP likely reflect some localised higher-energy processes. Deflation of the transported material following its deposition probably also contributed to the clast-supported nature of the pisolith-rich deposit.

POST-DEPOSITION

The matrix within the ABH in the test pits, the M2 excavation, and at the marketplace (Pollarolo *et al.* 2010: 6) is dominated by sand-sized grains and contains comparatively limited silt and very little clay, which contrasts the expected granulometry of a depocentre fed through slopewash that would tend to be dominated by sand and silt-sized grains (Selby 1994: 73). Additionally, the lateritic weathering of the dolerite bedrock would have produced considerably more clay and silt than is present in the sampled deposits (Widdowson 2007). The development of sand-dominated sediments of the ABH, within the context of the local lithology and formation processes, (Fig. 4) suggest they were winnowed of their silt- and clay-sized material after deposition. Together with the clast-supported nature of the ABH, the matrix and clast particle size distribution is indicative of the winnowing of the deposit by low-energy surface flow even in cases where clast density is comparatively low.

Mixing between the pisolith horizon and the ABH could have been caused by a range of turbatory processes before, during, and after the burial of the ABH (Wood & Johnson 1978; Mandel *et al.* 2017). The deflation of the ABH by slopewash during its

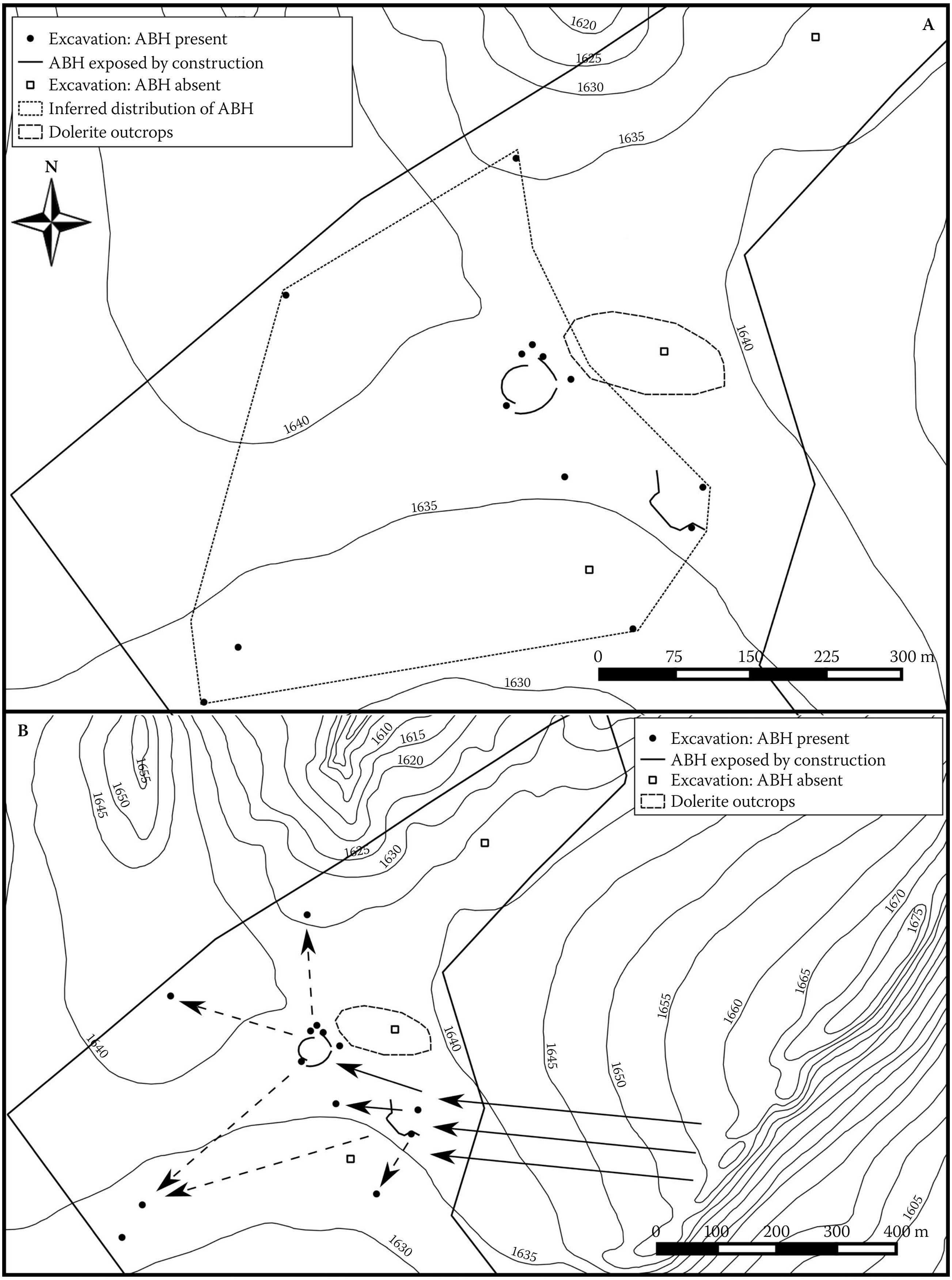

FIG. 11. *A) Topographic map of the study area indicating the locations where the artefact bearing horizon is known to be present or absent, and the inferred area of the Maropeng landscape covered by the artefact bearing horizon. B) A diagrammatic representation of the revised model for the movement of the sediment that formed the artefact-bearing horizon at Maropeng. The solid arrows indicate the movement of clast-bearing sediment from the ridge to the saddle. Dashed arrows indicate the subsequent movement of clast- and artefact-bearing sediment along the saddle and down the north and south sides of the saddle. Slopewash was the primary agent of transport and deposition in both cases.*

exposure would have reorganised the clasts as the deposit shifted from matrix-supported to clast-supported. Additionally, the matrix-supported pisolith-rich bands and pockets in the ABH at TPTP (Fig. 3) point to some pulses of variation in colluvial transport and deposition, with localised reworking of finer sediments (including pisoliths) in between periods of the deposition of coarser sediment. These finer deposits at TPTP underwent little or no deflation, but it is possible that if similar events occurred at other locations, and these deposits were winnowed and subsequently covered by coarser sediment (which was then also deflated), this would result in the inclusion of pisoliths in amongst the larger clasts in a clast-supported deposit.

Argilliturbation, the vertical movement of clasts driven by swelling and shrinking of clays due to seasonal changes in soil moisture (Wood & Johnson 1978; Mandel *et al*. 2017), is commonly associated with clay-rich soils. The very limited clay content of Facies 2 (Fig. 4) suggests that this is unlikely to have played a significant role, but it is possible that it may have had some impact if there were periods of landscape stability where the ABH sediments lay at the surface for a length of time prior to deflation.

After the burial of the deflated ABH and pisolith horizon, mixing may have occurred due to bioturbation (Wood & Johnson 1978; Mandel *et al*. 2017). No burrows or other soil structures associated with faunalturbation were identified in the field, but subsequent pedoturbation of the soil in Facies 3 and 4 would likely have obscured any evidence of this kind. Roots of grass and other small plants were commonly observed in Facies 3 and 4, and sometimes even in the upper portion of the ABH. Floralturbation is thus very likely to have played a role in any mixing.

The same turbatory processes may have been responsible for the steep dip of some clasts in the ABH, which is steeper than would be expected for accumulation by slopewash on relatively gentle slopes. Test pit locations where the ABH is 70 cm or more below the surface have markedly more gentle dip than those where the ABH is less than 50 cm deep, suggesting a combination of pedoturbative and bioturbative processes both mixed and rearranged the Facies 2 matrix and clasts.

M2 EXCAVATION

The fine and coarse sediments in the ABH at M2 have the same broad set of characteristics (including deposit fabric) as in the ABH across Maropeng. There is nothing to suggest a different process of deposition or any post-depositional processes not recorded in the test pits. The strongly planar nature of the fabric (Fig. 10) is consistent with deposition by run-off on a gentle slope, in contrast to the more linear fabrics associated with steeper surfaces (Lenoble & Bertran 2004; McPherron 2018). The generally gentle dip of natural and artefactual clasts suggests that their arrangement is largely the result of the winnowing of fines from the ABH and the retention of elements of the initial depositional fabric (Lenoble & Bertran 2004). However, the relatively high isotropy correlates well with that recorded in bioturbated colluvial deposits (Lenoble & Bertran 2004: fig. 16). The presence of pockets of non-winnowed fine sediment within the ABH shows the potential for variation in the local impacts of post-depositional processes across small areas in this context of deflation-driven pavement formation.

The ABH in M2 is significantly denser than in many of the test pits. This is likely due to its position a little upslope of the depocentre identified by Pollarolo *et al*. (2010) at the marketplace. The comparable thickness and density of the ABH in TPTP, some distance to the north, suggests that there were multiple locations (likely determined by variable local topography) on the landscape in which relatively large concentrations of clastic material were accumulated.

Of particular relevance to this study is the presence of pseudo-debitage created by the *in-situ* breakage of quartz and dolerite clasts caused by the compression of clastic material through the deflation and burial process (Fig. 6B). In several instances, quartz and dolerite clasts were exposed in the excavation that were broken with adjoining fragments still closely associated and exhibiting relatively fresh break surfaces. The complete lack of quartzite SFD (the dominant lithology for lithic production) may indicate the differential transport of smaller pieces or off-site knapping of the raw material. Therefore, the small quartz pieces in the M2 ABH are likely to be the product of post-depositional fracturing rather than preservation of SFD from lithic production. Small MSA and/or LSA artefacts were found in the upper facies at some test pit locations, and there is potential for mixing of these artefacts into the ABH through bioturbation. No artefacts of these types were recovered from the M2 excavation, but this possibility should be considered for any future excavations and lithic analysis at Maropeng.

HOMININ BEHAVIOUR

The heterogeneity in the abrasion states of artefacts across Maropeng (Figs 5 & 8) suggests that artefacts at each location were transported differing distances by natural processes before deposition. It is likely that the fresher artefacts were discarded by hominins nearer to these final depositional areas, while the more weathered ones were discarded at locations further away. Two locations (AFTP and HHTP) yielded artefacts that were larger than the largest natural clasts observed in these test pits (Table 1), suggesting these large artefacts are likely to have been discarded by hominins fairly near these locations and that they were affected by the deflation phase of deposit formation, but not extensive lateral movement.

These patterns, and the large spatial extent of the ABH, suggest that hominins discarded artefacts at multiple points on the landscape rather than at a single activity area. It is also clear from the evidence of clast transport and subsequent winnowing that the assemblage recovered from any specific location would contain artefacts of differing ages and initial discard locations. It is, therefore, very unlikely that the discard locations could be positively identified.

CONCLUSION

The ABH at Maropeng covers an area of at least 191 200 m² (Fig. 11A), considerably larger than initially proposed by Pollarolo *et al*. (2010). It may cover a larger area, particularly if it extends beyond TPTP, where it was particularly thick despite being on the edge of its known distribution. A localised discontinuity in the ABH is known to exist. It is possible that there are other absences in the form of depositional discontinuities or localised post-depositional removals of the ABH.

Based on the above discussion of the macroscopic and microscopic properties of the sediments at Maropeng, it is possible to propose the following site formation model.

Sediment that included both clasts and fines was transported onto the Maropeng landscape from the east. As the sediment came from the east and contains numerous quartzite clasts, it is most likely that it originated at the quartzite ridge (Fig. 11B). Some material was then washed down the slopes to the north and south of the saddle. Due to the gentle angle of the slopes below the ridge and the even gentler slopes to the south and the immediate north of the saddle, the material would have been transported by a (relatively) low energy slopewash. As the sediment was transported across the landscape, artefactual material at different locations on the surface was entrained and transported. The artefactual material was then deposited with the sediment.

Across much of Maropeng, the ABH was deposited onto pisolith-rich sediment. The deposited sediment was then winnowed by surface flow, during which the clasts were rearranged and compressed to form a clast-supported pavement with relatively coarse interstitial sediment. The compression of quartz clasts produced pieces that could be mistaken for SFD in some cases. The ABH was eventually buried under a layer of matrix-supported sediment, the thickness of which varies considerably. The northern slope steepens rapidly away from the saddle, and the ABH material is likely to have been eroded from most of this slope if it were originally deposited there.

Before, during, and after the burial of the ABH, mixing took place across the contact between the ABH and the underlying pisolith horizon as a result of a range of possible turbatory processes, including root action. Quartzite and quartz clasts moved down and mixed into the pisoliths, while some pisoliths moved up into the ABH. Clasts (including artefacts) may also have been mixed into the ABH from overlying sediments at some locations.

The results of this study indicate that Pollarolo *et al.*'s (2010) site formation model can, broadly speaking, be applied across the extent of the ABH at Maropeng. Their identification of slopewash as the primary depositional process and the quartzite ridge as the source of the natural sediment are both supported. However, their site formation model does not adequately address the effects of post-depositional processes and the variability in depositional (and post-depositional) processes across the landscape. The model developed from the current research refines the existing hypothesis to address both factors.

The variation in sedimentary and geomorphological properties of the ABH across Maropeng is considerable. This means that, while the general site formation model outlined above gives broad geoarchaeological context to the ABH, it will not provide acceptable context to any specific location. The interpretation of artefacts yielded from any particular location will require fine-scale analysis of site formation in order to identify the specific processes that have affected the deposit there, and how, and to what degree, they may have impacted the assemblage.

The evidence from M2 indicates that the lithic artefacts recovered from there were transported varying distances by slopewash. Therefore, they are in secondary context and represent human activities taking place at different points on the landscape. These artefacts accumulated over an unknown length of time, with a palimpsest being formed as the deposit was deflated and artefacts of different ages were incorporated into a single horizon. In addition to being mixed, the assemblage was modified by the removal of some artefacts due to differential transport and the winnowing of the deposit. Therefore, the M2 assemblage is both incomplete and the averaged product of human actions over time and space. This has implications for what approach is applied to the analysis of the assemblage, and what interpretations can be made, but it does not mean that this assemblage is not informative, especially given the rarity of Early Acheulean deposits in southern Africa (Moll 2017).

Attempts to date samples collected from above and below the ABH with optically stimulated luminescence have proven unsuccessful. The lack of maximum and minimum ages prevents a meaningful estimate of how long it took for the artefacts in the ABH to accumulate and thus, how much time has been telescoped down into the recovered assemblages. This has implications for both behavioural interpretations and understanding how the development of the Maropeng landscape fits into broader regional environmental and geomorphic patterns. The application of different techniques, such as electron spin resonance of quartz grains, could provide age estimates in future.

Spatial patterns in artefact abrasion across Maropeng indicate that artefacts were deposited by hominins at many locations across the landscape, rather than just at the quartzite ridge from which the natural clasts within the ABH originated. Therefore, despite the modification of the ABH assemblages by sedimentological processes, they provide evidence for the use of the landscape by hominins during the Early Acheulean.

ACKNOWLEDGEMENTS

The Palaeontological Scientific Trust (PAST) provided funding for PM's Honours research project, which forms the basis of much of the research presented here. The support of GENUS: DSI-NRF Centre of Excellence in Palaeosciences (Grant 86073) towards this research is acknowledged. DS would like to thank Maropeng management, in particular, Lindsay Marshall, for their permission to conduct research on the property and their support in hosting various field schools taught at the site.

NOTES

[1] The term 'clast' is used to refer to both natural clasts and artefacts, unless specified otherwise.

[2] The term 'horizon' is used here in the geological sense (i.e. a distinctive laterally continuous layer, often marked by the presence of a particular sedimentary component or biological or artefactual inclusion), and does not imply that the ABH should be considered a soil horizon.

REFERENCES

Benn, D.I. 1994. Fabric shape and the interpretation of sedimentary fabric data. *Journal of Sedimentary Research* 64: 910–915.

Bertran, P. & Texier, J-P. 1995. Fabric analysis: application to Paleolithic sites. *Journal of Archaeological Science* 22(4): 521–535.

Bluck, B.J. 1987. Bed forms and clast size changes in gravel-bed rivers. In: Richards, K. (ed.) *River Channels: Environment and Process*: 159–178. Oxford: Basil Blackwell.

Blumenschine, R.J. & Masao, F.T. 1991. Living sites at Olduvai Gorge, Tanzania? Preliminary landscape archaeology results in the basal Bed II lake margin zone. *Journal of Human Evolution* 21(6): 451–462.

Blumenschine, R.J., Masao, F.T., Tactikos, J.C. & Ebert, J.I. 2008. Effects of distance from stone source on landscape-scale variation in Oldowan artifact assemblages in the Paleo-Olduvai Basin, Tanzania. *Journal of Archaeological Science* 35(1): 76–86.

Bourman, R.P. 1993. Perennial problems in the study of laterite: a review. *Australian Journal of Earth Sciences* 40(4): 387–401.

Brain, C.K. 1993. Structure and stratigraphy of the Swartkrans Cave in the light of the new excavations. In: Brain, C.K. (ed.) *Swartkrans: A Cave's Chronicle of Early Man*: 23–33. Pretoria: Transvaal Museum.

Braun, D.R., Rogers, M.J., Harris, J.W. & Walker, S.J. 2008. Landscape-scale variation in hominin tool use: evidence from the Developed Oldowan. *Journal of Human Evolution* 55(6): 1053–1063.

Butzer, K.W. 1974. Geo-archeological interpretation of Acheulian calc-pan sites at Doornlaagte and Rooidam (Kimberley, South Africa). *Journal of Archaeological Science* 1(1): 1–25.

Butzer, K.W. 1988. Sedimentological interpretation of the Florisbad spring deposits, South Africa. *Palaeoecology of Africa and the Surrounding Islands* 19: 181–189.

Caruana, M.V. 2017. Lithic production strategies in the Oldowan assemblages from Sterkfontein Member 5 and Swartkrans Member 1, Gauteng province, South Africa. *Journal of African Archaeology* 15(1): 1–19.

Caruana, M.V., Tasker, D. & Stratford, D.J. 2019. Identifying raw material transportation and reduction strategies from the lithic scatters at Elandsdrift Farm (Cradle of Humankind World Heritage Site), South Africa. *African Archaeological Review* 36(2): 271–289.

Catuneanu, O. & Eriksson, P.G. 2002. Sequence stratigraphy of the Precambrian Rooihoogte–Timeball Hill rift succession, Transvaal Basin, South Africa. *Sedimentary Geology* 147(1–2): 71–88.

Cawthorn, R.G. 2015. The Bushveld Complex, South Africa. In: Charlier, B., Namur, O., Latypov, R. & Tegner, C. (eds) *Layered Intrusions*: 517–587. Dordrecht: Springer Geology.

Cawthorn, R.G., Davies, G., Clubley-Armstrong, A. & McCarthy, T.S. 1981. Sills associated with the Bushveld Complex, South Africa: an estimate of the parental magma composition. *Lithos* 14(1): 1–16.

Eriksson, P.G., Schweitzer, J.K., Bosch, P.J.A., Schreiber, U.M., Van Deventer, J.L. & Hatton, C.J. 1993. The Transvaal Sequence: an overview. *Journal of African Earth Sciences* 16: 25–51.

Evans, D.J.A. 2000. A gravel outwash/deformation till continuum, Skalafellsjökull, Iceland. *Geografiska Annaler, Series A, Physical Geography* 82: 499–512.

Goldberg, P., Berna, F. & Chazan, M. 2015. Deposition and diagenesis in the Earlier Stone Age of Wonderwerk Cave, Excavation 1, South Africa. *African Archaeological Review* 32: 613–643

Goldberg, P. & MacPhail, R.I. 2006. *Practical and Theoretical Geoarchaeology*. Oxford: Blackwell Publishing.

Goldberg, P., Rhodes, S.E. & Chazan, M. 2023. Geological and archaeological insight into site formation processes and Acheulean occupation at Wonderwerk Cave, Northern Cape Province, South Africa. *Journal of Paleolithic Archaeology* 6(1): 33.

Gomez, B., Dowdeswell, J.A. & Sharp, M. 1988. Microstructural control of quartz sand grain shape and texture: implications for the discrimination of debris transport pathways through glaciers. *Sedimentary Geology* 57(1–2): 119–129.

Herries, A.I., Arnold, L.J., Boschian, G., Blackwood, A.F., Wilson, C., Mallett, T., Armstrong, B., Demuro, M., Petchey, F., Meredith-Williams, M., Penzo-Kajewski, P. & Caruana, M.V. 2022. A marine isotope stage 11 coastal Acheulian workshop with associated wood at Amanzi Springs Area 1, South Africa. *PLoS One* 17: e0273714.

Kandel, A.W., Felix-Henningsen, P. & Conard, N.J. 2003. An overview of the spatial archaeology of the Geelbek Dunes, Western Cape, South Africa. In: Füleky, G. (ed.) *Papers of the 1st International Conference on Archaeology and Soils*: 37–44. Oxford: BAR Publishing.

Kuman, K. 1994. The archaeology of Sterkfontein – past and present. *Journal of Human Evolution* 27: 471–495.

Kuman, K. 1998. The earliest South African Industries. In: Petraglia, M.D. & Korisettar, R. (eds) *Early Human Behaviour in Global Context: The Rise and Diversity of the Lower Palaeolithic Record*: 151–186. London: Routledge.

Kuman, K. 2003. Site formation in the early South African Stone Age sites and its influence on the archaeological record. *South African Journal of Science* 99: 251–254.

Kuman, K. 2007. The Earlier Stone Age in South Africa: site context and the influence of cave studies. In: Pickering, T.R., Schick, K. & Toth, N. (eds) *Breathing Life into Fossils: Taphonomic Studies in Honor of C.K. (Bob) Brain*: 181–198. Gosport: Stone Age Institute Press.

Kuman, K. 2016. Development of the archaeological record in southern Africa during the Earlier Stone Age. In: Knight, J. & Grab, S. (eds) *Quaternary Environmental Change in Southern Africa: Physical and Human Dimensions*: 349–370. Cambridge: Cambridge University Press.

Kuman, K. & Field, A.S. 2009. The Oldowan Industry from Sterkfontein Caves, South Africa. In: Schick, K. & Toth, N. (eds) *The Cutting Edge: New Approaches to the Archaeology of Human Origins*: 151–169. Gosport: Stone Age Institute Press.

Kuman, K. & Gibbon, R.J. 2018. The Rietputs 15 site and Early Acheulean in South Africa. *Quaternary International* 480: 4–15.

Kuman, K., Sutton, M.B., Pickering, T.R. & Heaton, J.L. 2018. The Oldowan industry from Swartkrans cave, South Africa, and its relevance for the African Oldowan. *Journal of Human Evolution* 123: 52–69.

Lascelles, D.F. 2016. The origin of terrestrial pisoliths and pisolitic iron ore deposits: raindrops and sheetwash in a semi-arid environment. *Sedimentary Geology* 341: 232–244.

Lenoble, A. & Bertran, P. 2004. Fabric of Palaeolithic levels: methods and implications for site formation processes. *Journal of Archaeological Science* 31(4): 457–469.

Leyland, R.C. 2008. Vulnerability mapping in Karst terrains, exemplified in the wider Cradle of Humankind World Heritage Site. Unpublished MSc dissertation. Pretoria: University of Pretoria.

Lotter, M.G. 2020. Stuck in a loop: investigating fabric patterns in the Stone Age gravel sequence at Canteen Kopje, Northern Cape Province, South Africa. *Transactions of the Royal Society of South Africa* 75(1): 64–77.

Lotter, M.G., Gibbon, R.J., Kuman, K., Leader, G.M., Forssman, T. & Granger, D.E. 2016. A geoarchaeological study of the Middle and Upper Pleistocene levels at Canteen Kopje, Northern Cape Province, South Africa. *Geoarchaeology* 31: 304–323.

Lotter, M.G. & Kuman, K. 2018. The Acheulean in South Africa, with announcement of a new site (Penhill Farm) in the lower Sundays River Valley, Eastern Cape Province, South Africa. *Quaternary International* 480: 43–65.

Lukich, V., Cowling, S. & Chazan, M. 2020. Palaeoenvironmental reconstruction of Kathu Pan, South Africa, based on sedimentological data. *Quaternary Science Reviews* 230: 106153.

Mandel, R.D., Goldberg, P. & Holliday, V.T. 2017. Site formation processes. In: Gilbert, A.S., Goldberg, P., Holliday, V.T., Mandel, R.D. & Sternberg, R.S. (eds) *Encyclopedia of Geoarchaeology:* 797–817. Dordrecht: Springer.

Martini, J.E.J., Wipplinger, P.E., Moen, H.F.G. & Keyser, A. 2003. Contribution to the speleology of Sterkfontein Cave, Gauteng Province, South Africa. *International Journal of Speleology* 32(1): 43–69.

Matmon, A., Ron, H., Chazan, M., Porat, N. & Horwitz, L.K. 2012. Reconstructing the history of sediment deposition in caves: a case study from Wonderwerk Cave, South Africa. *Geological Society of America Bulletin* 124(3–4): 611–625.

Maurin, T., Bertran, P., Delagnes, A. & Boisserie, J.R. 2017. Early hominin landscape use in the Lower Omo Valley, Ethiopia: insights from the taphonomical analysis of Oldowan occurrences in the Shungura Formation (Member F). *Journal of Human Evolution* 111: 33–53.

Mazzullo, J. & Graham, A.G. 1988. *Handbook for Shipboard Sedimentologists*. College Station, TX: Ocean Drilling Program, Texas A&M University.

McPherron, S.J.P. 2005. Artifact orientations and site formation processes from total station proveniences. *Journal of Archaeological Science* 32(7): 1003–1014.

McPherron, S.J.P. 2018. Additional statistical and graphical methods for analyzing site formation processes using artifact orientations. *PloS One* 13: e0190195.

Mercador, J., Martí, R., Martínez, J.L. & Brooks, A. 2002. The nature of 'stone-lines' in the African Quaternary record: archaeological resolution at the rainforest site of Mosumu, Equatorial Guinea. *Quaternary International* 89: 71–96.

Mills, H.H. 1983. Clast-fabric strength in hillslope colluvium as a function of slope angle. *Geografiska Annaler. Series A, Physical Geography* 65: 255–262.

Moll, R. 2017. A technological study of the lithic artefacts from the Earlier Stone Age Site of Maropeng, Cradle of Humankind, South Africa. Unpublished MSc dissertation. Johannesburg: University of the Witwatersrand.

Morrissey, P. 2015. A geoarchaeological investigation of the Earlier Stone Age site at Maropeng in the Cradle of Humankind. Unpublished Honours dissertation. Johannesburg: University of the Witwatersrand.

Obbes, M.A. 2000. The structure, stratigraphy and sedimentology of the Black Reef-Malmani-Rooihoogte succession of the Transvaal supergroup south-west of Pretoria. *Council for Geoscience Bulletin* 127.

Oestmo, S., Schoville, B.J., Wilkins, J. & Marean, C.W. 2014. A Middle Stone Age paleoscape near the Pinnacle Point caves, Vleesbaai, South Africa. *Quaternary International* 350: 147–168.

Petraglia, M.D. & Potts, R. 1994. Water flow and the formation of Early Pleistocene artifact sites in Olduvai Gorge, Tanzania. *Journal of Anthropological Archaeology* 13: 228–254.

Phillips, N., Moffat, I., Mackay, A. & Jones, B.G. 2023. The sedimentary context of open-air archaeology: a case study in the Western Cape's Doring River Valley, South Africa. *Soil Systems* 7(1): 25.

Plummer, T. 2004. Flaked stones and old bones: biological and cultural evolution at the dawn of technology. *Yearbook of Physical Anthropology* 47: 118–164.

Pollarolo, L., Susino, G., Kuman, K. & Bruxelles, L. 2010. Acheulean artefacts at Maropeng in the Cradle of Humankind World Heritage Site, Gauteng Province, South Africa. *South African Archaeological Bulletin* 65: 3–12.

Potts, R. 1991. Why the Oldowan? Plio-Pleistocene toolmaking and the transport of resources. *Journal of Anthropological Research* 47: 153–176.

Powers. M.C. 1953. A new roundness scale for sedimentary particles. *Journal of Sedimentary Petrology* 23: 117–119.

Price Williams, D., Watson, A. & Goudie, A.S. 1982. Quaternary colluvial stratigraphy, archaeological sequences and palaeoenvironment in Swaziland, southern Africa. *The Geographical Journal* 148(1): 50–67.

Pye, K. 1994. Properties of sediment particles. In: Pye, K. (ed.) *Sediment Transport and Depositional Processes*: 1–24. Oxford: Blackwell Scientific Publications.

Rapp, G. & Hill, C.L. 1998. *Geoarchaeology: The Earth-Science Approach to Archaeological Interpretation*. New Haven: Yale University Press.

Sarkar, T., Mishra, M. & Chatterjee, S. 2020. On detailed field-based observations of laterite and laterization: a study in the Paschim Medinipur lateritic upland of India. *Journal of Sedimentary Environments* 5(2): 219–245.

Schick, K.D. 1987. Modeling the formation of Early Stone Age artifact concentrations. *Journal of Human Evolution* 16: 789–807.

Selby, M.J. 1994. Hillslope sediment transport and deposition. In: Pye, K. (ed.) *Sediment Transport and Depositional Processes*: 61–87. Oxford: Blackwell Scientific Publications.

Shakesby, R.A. & Whitlow, R. 1991. Perspectives on prehistoric and recent gullying in central Zimbabwe. *GeoJournal* 23: 49–58.

Shea, J.J. 1999. Artifact abrasion, fluvial processes, and "living floors" from the Early Paleolithic site of 'Ubeidiya (Jordan Valley, Israel). *Geoarchaeology* 14(2): 191–207.

Stein, J.K. 1985. Interpreting sediments in cultural settings. In: Stein, J.K. & Farrand, W.R. (eds) *Archaeological Sediments in Context*: 5–20. Orono: Center for the Study of Early Man.

Stocking, M.A. 1978. Interpretation of stone-lines. *South African Geographical Journal* 60(2): 121–134.

Stratford, D.J. 2011. The underground central deposits of the Sterkfontein Caves, South Africa. Unpublished PhD thesis. Johannesburg: University of the Witwatersrand.

Stratford, D. 2017. A review of the geomorphological context and stratigraphy of the Sterkfontein Caves, South Africa. In: Klimchouk, A., Palmer, A.N., De Waele, J., Auler, A.S. & Audra, P. (eds) *Hypogene Karst Regions and Caves of the World*: 879–891.Cham: Springer.

Stratford, D.J., Bruxelles, L., Clarke, R.J. & Kuman, K. 2012. New stratigraphic interpretations of the fossil and artefact-bearing deposits of the Name Chamber, Sterkfontein. *South African Archaeological Bulletin* 67(196): 159–167.

Stratford, D.J., Grab, S. & Pickering, T.R. 2014. The stratigraphy and formation history of fossil- and artefact-bearing sediments at the Milner Hall, Sterkfontein Cave, South Africa: new interpretations and implications for palaeoanthropology and archaeology. *Journal of African Earth Sciences* 96: 155–167.

Sutton, M.B., Pickering, T.R., Pickering, R., Brain, C.K., Clarke, R.J., Heaton, J.L. & Kuman, K. 2009. Newly discovered fossil-and artifact-bearing deposits, uranium-series ages, and Plio-Pleistocene hominids at Swartkrans Cave, South Africa. *Journal of Human Evolution* 57: 688–696.

Tasker, D. 2020. Raw material sourcing and economy from the Acheulean open-air site of Maropeng, Cradle of Humankind, South Africa. Unpublished MSc dissertation. Johannesburg: University of the Witwatersrand.

Taylor, G. & Eggleton, R.A. 2008. Genesis of pisoliths and of the Weipa bauxite deposit, northern Australia. *Australian Journal of Earth Sciences* 55: S87–S103.

Taylor, G., Eggleton, R.A., Foster, L.D. & Morgan, C.M. 2008. Nature of the Weipa Bauxite deposit, northern Australia. *Australian Journal of Earth Sciences* 55: S45–S70.

Thorne, R., Anand, R. & Suvorova, A. 2014. The formation of fluvio-lacustrine ferruginous pisoliths in the extensive palaeochannels of the Yilgarn Craton, Western Australia. *Sedimentary Geology* 313: 32–44.

Toffolo, M.B., Brink, J.S. & Berna, F. 2019. Microstratigraphic reconstruction of formation processes and paleoenvironments at the Early Pleistocene Cornelia-Uitzoek hominin site, Free State Province, South Africa. *Journal of Archaeological Science: Reports* 25: 25–39.

Watson, A., Price Williams, D. & Goudie, A.S. 1984. The palaeoenvironmental interpretation of colluvial sediments and palaeosols of the Late Pleistocene Hypothermal in southern Africa. *Palaeogeography, Palaeoclimatology, Palaeoecology* 45(3–4): 225–249.

Widdowson, M. 2007. Laterite and ferricrete. In: Nash, D.J. & McLaren, S.J. (eds) *Geochemical Sediments and Landscapes*: 46–94. Oxford: Blackwell Publishing.

Will, M., Blessing, M., Möller, G.H.D, Msimanga, L., Pehnert, H., Riedesel, S., Botha, G.A. & Sommer, C. 2024. The Jojosi Dongas: an interdisciplinary project to study the evolution of human behaviour and landscapes in open-air contexts. *Southern African Field Archaeology* 19: 3010.

Wood, W.R. & Johnson, D.L. 1978. A survey of disturbance processes in archaeological site formation. *Advances in Archaeological Method and Theory* 1: 315–381.

Wroth, K., Tribolo, C., Bousman, C.B., Horwitz, L.K., Rossouw, L., Miller, C.E. & Toffolo, M.B. 2022. Human occupation of the semi-arid grasslands of South Africa during MIS 4: new archaeological and paleoecological evidence from Lovedale, Free State. *Quaternary Science Reviews* 283: 107455.